Measurements of Snow Depths Using the Geometry-free Linear Combinations of the two L-band Phases from GPS Satellites

Masaru Ozeki

Space Geodesy Research Section
Earth and Planetary Dynamics, Dept. Natural History Sci.
Graduate School of Science, Hokkaido University

8 February, 2011

Contents

Abstract

Geometry-free linear combination (often called L4) is the difference between the phases of two carrier frequencies, L1 (1.5 GHz) and L2 (1.2 GHz), used in Global Positioning System (GPS). L4 is often used to study ionospheric total electron contents (TEC) because it depends only on the delays caused by electrons in ionosphere (i.e. all other geometric factors are cancelled by taking the difference in L1 and L2 phases). In this study, I report a new application of L4, i.e. measurement of snow depths, by analyzing multipath signatures in data from a dense GPS array, GEONET (GPS Earth Observation Network) in Japan.

Multipath is the interference between direct and reflected waves from GPS satellites. Because multipath causes error in positioning, GPS antennas are designed to reduce such reflected waves. Larson et al. (2008) first suggested that multipath signature could be utilized to measure physical status of the ground surface as a reflector, e.g. soil moisture. They further proposed methods to measure snow depths (Larson et al., 2009), and vegetation (Small et al., 2010) using multipath.

As a GPS satellite moves in the sky, the change in its elevation angle lets excess path length vary slowly in time. Thus, temporal changes in the L1 / L2 phases of reflected waves make the amplitude and phase of the sum of the direct and the reflected waves fluctuate in particular periods. Such multipath-signatures become larger when the satellite becomes lower. The fluctuation periods depend on the antenna height, i.e. an antenna with smaller height shows a longer period (because the change of excess path length gets slower). Because snow causes apparent reduction in antenna height, phase/amplitude fluctuation periods can be used to constrain the snow depth.

These past studies used signal-to-noise ratio (SNR) to measure fluctuations in amplitudes caused by multipath. Here I report a new method to measure snow depth in using fluctuations in phase. I also show that L4 is appropriate for this purpose because it is geometry-free. Here I analyzed data at a GEONET site 02877 in Shinshinotsu, NE of Sapporo, Hokkaido, Japan, from January to April in 2009. Snow depths measured with SNR and L4 were found to agree well. Such data are also compared with those measured by an AMeDAS (Automatic Meteorological Data Acquisition System) ultrasonic snow depth sensor, located ~500 m to the west. They also agreed with each other fairly well. In many networks, raw GPS data open to public do not include SNR information. However, L4 can always be made available by combining L1 and L2 phases. This study demonstrates that L4 can be used to analyze multipath as a proxy when SNR data are not available.

概要

Geometry-free linear combination（幾何学的要素が含まれない線形結合、しばしばL4と呼ばれる）とは、全地球測位システム（Global Positioning System, GPS）で使われる二つの搬送波、L1（1.5 GHz）とL2（1.2 GHz）の位相の単純な差である。L4は電離圏の電子数によって生じる遅延にのみに依存するため（他のすべての幾何学的要素はL1とL2位相の差をとった時点で取り除かれている)、しばしば電離圏の総電子数を観測するために使われる。本研究では、日本の稠密GPS網（GPS Earth Observation Network, GEONET）から得られるデータのマルチパス信号を解析することで、積雪深度を計測するというL4の新しい活用法について報告する。

マルチパスとはGPS衛星からの直接波と反射波の干渉によって起こる様々な現象のことである。マルチパスは測位誤差をもたらすため、GPSアンテナは反射波の影響をなるべく受けないように設計されている。Larson et al.（2008）は、マルチパス信号が地面の物理的な状態、例えば土壌水分量を測定するのに利用できることを初めて報告した。彼女らはさらにマルチパスを使うことで積雪深度（Larson et al., 2009）や植生（Small et al., 2010）を測定する方法を提案した。

GPS衛星が上空を移動し仰角が変化するに従って、余分光路長はゆっくりと時間変化する。受信機で観測されるのは直接波と反射波を足し合わせたものであるが、このように反射波のL1 / L2位相が時間変化すると受信された信号の振幅と位相は特定の周期で変動する。その周期はアンテナ高に依存し、アンテナが低い程周期は長くなる（余分光路長の変化が緩慢になるため)。マイクロ波の多くは雪面で反射されるため、降雪は見かけのアンテナ高を低くする。反射波は衛星の仰角が低い時に強くなる。従って地平線に上った直後や沈む直線のGPS衛星の受信電波の位相/振幅の振動周期を解析すると積雪深度を特定することができるのである。

Larson et al.（2009）はマルチパスによって生じる振幅の振動をS/N比（Signal-to-Noise Ratio, SNR）を使って計測した。本研究ではL4の位相の振動を使って（L4はgeometry-freeであるためこの目的に適している）積雪深度を測定するという新しい方法を開発した。今回は、日本の北海道石狩郡新篠津村にあるGEONET GPS局（02877）の2009年1月から4月にかけてのデータを解析した。SNRとL4で測定された積雪深度は良く一致することが分かった。これらの積雪深度はまた、西に約500m離れた所にあるアメダス(Automatic Meteorological Data Acquisition System, AMeDAS）超音波積雪深度計によって測定された積雪深度とも良く一致した。世界中の多くのGPSネットワークでは、一般向けに公開されている生のGPSデータの中にSNRの情報を含んでいない。しかしながら、L4はL1とL2の位相差でありいつでも利用することができる。本研究はSNRデータが利用できない時にL4がマルチパスの解析するために実用に耐えることを明らかにした。

1 Introduction

In conventional snow depth meters, the snow depths are measured from the round trip times of ultrasonic waves reflected by the snow surface (Fig. 1.1). In this study, I developed a new method to measure snow depths by observing Global Positioning System (GPS) multipaths (Fig. 1.2). Multipath is the interference between direct microwaves from GPS satellites and those reflected somewhere, and causes, e.g. measurement errors repeating every sidereal day (the orbital period of the satellites is a half sidereal day). Larson et al. (2009) recently reported a method to measure the snow depths using multipath. They used signal-to-noise ratio (SNR) to measure interference between the direct and reflected waves. Here we tried to use geometry-free linear combination (often called L4), which does not depend on coordinates of GPS sites and satellites, or atmospheric delays.

In this chapter, I briefly overview GPS and L4.

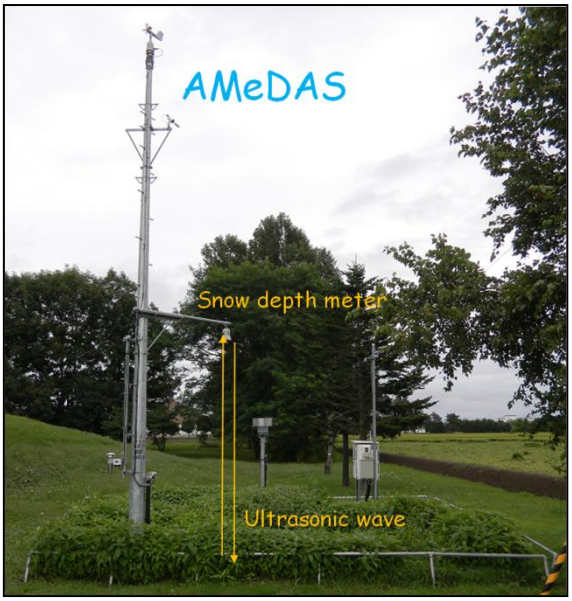

Figure. 1.1 : Ultrasonic snow depth sensor in AMeDAS (Automatic Meteorological Data Acquisition System) run by the Japan Meteorological Agency.

Figure. 1.2 : GEONET GPS station at the site 950128 in Fujino, Minami-ku, Sapporo-city.

1.1 GPS

GPS is a positioning system using satellites, and has been developed using over 100 billion dollars of budget by the United States government for over 20 years. GPS satellites started to be launched by the U.S. Department of Defense in 1978, and have been in full operation since 1993, with ~30 satellites in orbits of periods ~12 hours (20,000 km in altitude). By receiving microwave signals from these satellites, we can know coordinates of the receiver and precise time. GPS was a system developed originally for military navigational aid. However, GPS nowadays has been increasingly used by civilian users for, e.g., automotive navigation, operational control of ships and aircraft, measurement of tectonic movements, constituting a part of the global information infrastructure.

GPS system consists of the space section, the user section, and the control section. In the following, I briefly explain the space and user sections.

Space section (satellite)

GPS satellites consist of 24 satellites in total (~30 satellites if spares are included). They are deployed in six different orbital planes with angular separation of 60-degrees in Ω (longitude of ascending node). Thus it is ensured worldwide that at least four satellites always exist above the horizon. The orbital eccentricity e is 0 to 0.01, i.e. nearly circular orbits. The semimajor axis a is about 26,600 km, and these satellites revolve around the earth with a period of 11 hours 58 minutes (0.5 sidereal day). Because one solar day is 24 hours, same constellation pattern of the satellites appears earlier by ~4 minutes than the previous day..

GPS satellites are equipped with atomic clocks (cesium and rubidium clock) which have high stability as frequency standard. Fundamental frequency f_0 (= 10.23 MHz) of this atomic clock is multiplied by 154 and 120, to make carrier waves of L1 and L2 frequencies, respectively. However, actual f_0 is 0.00455 Hz lower than 10.23 MHz due to relativistic corrections coming from the higher gravity potential of the orbit than the Earth's surface.

Although all the satellites send the same frequencies of L1 and L2, they do not interfere with each other because their signals are modulated by Pseudo Random Noise (PRN) of unique to individual satellites. PRN has publicly available C/A (Coarse/Acquisition) code, and military P (Protected) code. The former consists of a series of binary codes (0 or 1) as long as 1023 bit, repeating every microsecond. There

are 36 different C/A code patterns in total. The period of P code is 37 weeks, but has been divided into parts as long as a week and assigned to each satellite (Table. 1.1).

Table. 1.1 : Frequencies and wavelengths of the carrier and code used in GPS (Tsuji, 1998)

carrier		C/A code	P code
L1	1575.42 Mhz (19.0 cm)	1.023 MHz (293 m)	10.23 MHz (29.3 m)
L2	1227.60 Mhz (24.4 cm)	non	10.23 MHz (29.3 m)

User section (GPS receiver)

A GPS receiver consists of an antenna to receive signals from GPS satellites and the receiver itself to decode and encode the signals. A simple receiver for navigation reproduces the C/A code (or P code) pattern similar to satellites, and shift the reproduced C/A code in time until the maximum correlation with the received C/A code is obtained. The obtained time shift corresponds to the time required for the microwave to travel from the satellite to the receiver. Therefore, by multiplying this time by speed of light, the distance between the satellite and the receiver is obtained. However, it is difficult to fully synchronize the receiver clock to the satellite clock, and the measured distance has an error due to the receiver clock offset. This is why the measured quantity is called “pseudo” range. Actually, we obtain such pseudo ranges using four or more satellites, and estimate the clock offset in addition to the receiver coordinates.

In a GPS receiver for precise geodetic purposes, we use carrier phases, instead of codes, to determine site coordinates. The received signals are phase-modulated by the code and their carrier phases cannot be measured precisely. However, after successful decoding, the original sine waves of the L1 and L2 frequencies are recovered in the receiver and we can measure phases. When we use carrier phases for precise positioning, measured phases have integer ambiguities. Such ambiguities are normally estimated as parameters together with other geodetic parameters.

1.2 Geometry-free linear combination (L4)

In the upper atmosphere (thermosphere), some of the atmospheric atoms and molecules ionize by ultraviolet solar radiation. So this layer is often called as ionosphere. Electrons in the ionosphere cause the delay in propagation of two microwaves, L1 and L2. Because the ionospheric delay is inversely proportional to the square of the frequency, we can know such ionospheric delays by receiving the two microwaves simultaneously. For normal geodetic use of GPS, we make an "ionosphere-free" linear combination (often called L3) of L1 and L2 by

$$L3 = f_1^2 / (f_1^2 - f_2^2)\, L1 - f_2^2 / (f_1^2 - f_2^2)\, L2 \quad (1.1)$$

, where f_1 and f_2 are the frequencies of the L1 and L2 carriers, respectively. In this equation observed phases are multiplied by wave lengths, so L1 and L2 have unit of length (m). On the other hand, another linear combination, or the simple difference between L1 and L2 (often called L4), has ionospheric information only, i.e. other geodetic information (e.g., neutral atmosphere delay, GPS satellite position and GPS site position) are cancelled by taking the difference. So this value is called geometry-free combination.

$$L4 = L1 - L2 \quad (1.2)$$

L4 is proportional to the number of electrons integrated along the line of sight, and is frequently used to study the ionosphere and its disturbances.

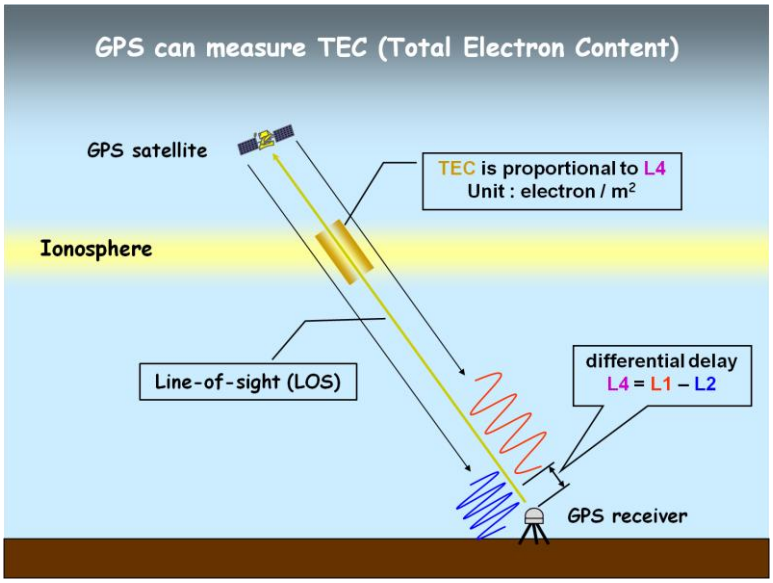

Figure. 1.3 : L4 is the difference between L1 and L2, and is proportional to the TEC, number of electrons integrated along the line-of-sight.

2 Principles of GPS snow depth meter

2.1 GPS antenna height (snow depth) dependence of multipath phase

Multipath is the interference between direct and reflected waves from GPS satellites. According to the model by Eloségui et al. (1995), multipath contribution to phase can be represented by

$$\delta\phi(\varepsilon;\alpha,H,\lambda) = \tan^{-1}\frac{\alpha\sin\left[4\pi\frac{H}{\lambda}\sin\varepsilon\right]}{1+\alpha\cos\left[4\pi\frac{H}{\lambda}\sin\varepsilon\right]} \quad (2.1)$$

, where ε is the satellite elevation angle, α is reflectivity of the ground, H is GPS antenna height and λ is the wavelength (Fig. 2.1).

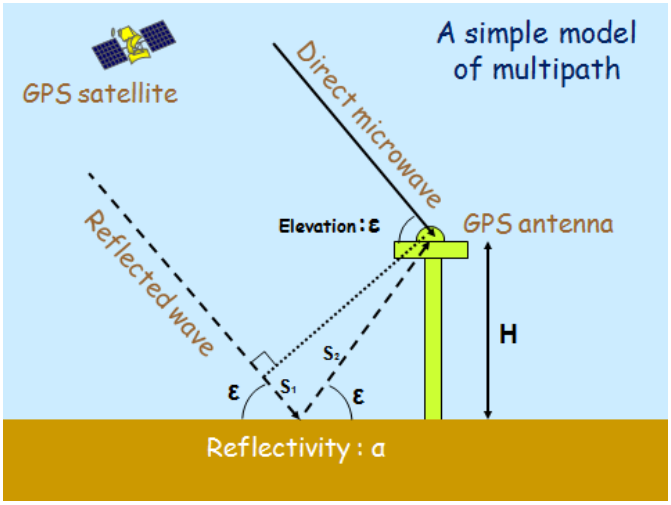

Figure. 2.1 : A simple model of multipath (Eloségui et al., 1995). The excess path length of the reflected wave is equal to the sum of S_1 and S_2.

As the GPS satellite moves in the sky, elevation changes, and L1 / L2 (and L4 also) phases of reflected waves also change in particular periods. Such multipath-origin phase fluctuation shows large amplitudes when the satellite is low. The fluctuation periods depend on the antenna height, i.e. an antenna with smaller height shows a longer period (because the change of excess path length gets slower). Thus multipath period can be used to constrain the depth of snow, which causes apparent reduction in antenna height (Fig. 2.3-5). In our software, we converted the unit of L4 to TECU (TEC

unit, 10^{16} electrons/m^2) because the software is originally designed to study ionospheric disturbances. Because it is the multipath frequency peak that is important, this conversion doesn't affect the observation of snow depths by GPS.

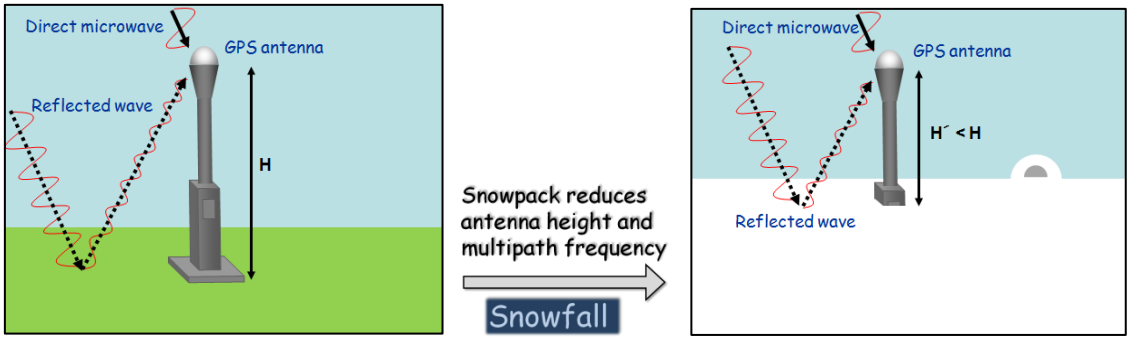

Figure. 2.2 : The situation around a GPS antenna before and after snow accumulation. Snow pack reduces apparent antenna height from H to H', which also modifies changing rates of the excess path length.

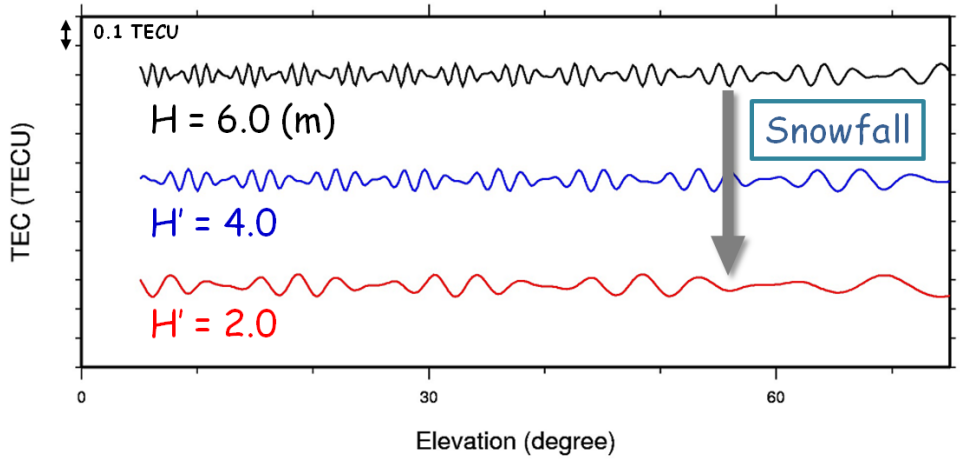

Figure. 2.3 : Modeled fluctuation of L4 phase (in terms of TEC) due to multipath to the elevation of the satellite. Because snowpack reduces antenna height, phase fluctuation becomes slower.

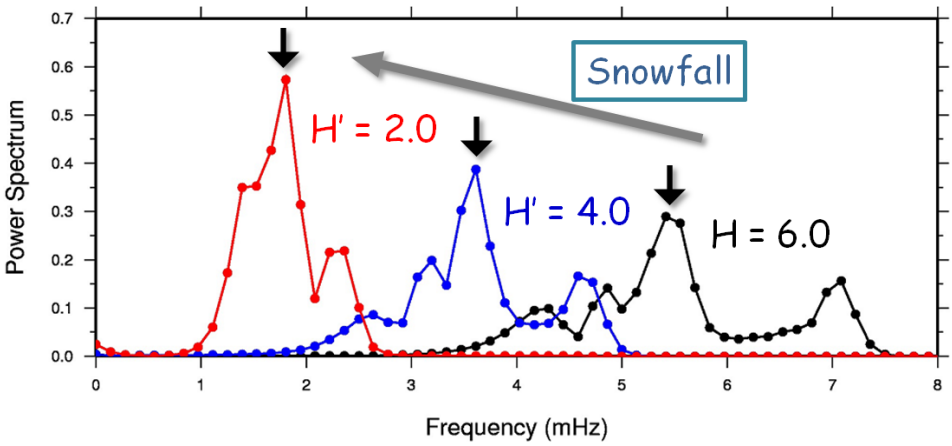

Figure. 2.4 : Spectrogram of the TEC fluctuations in Figure. 2.3.

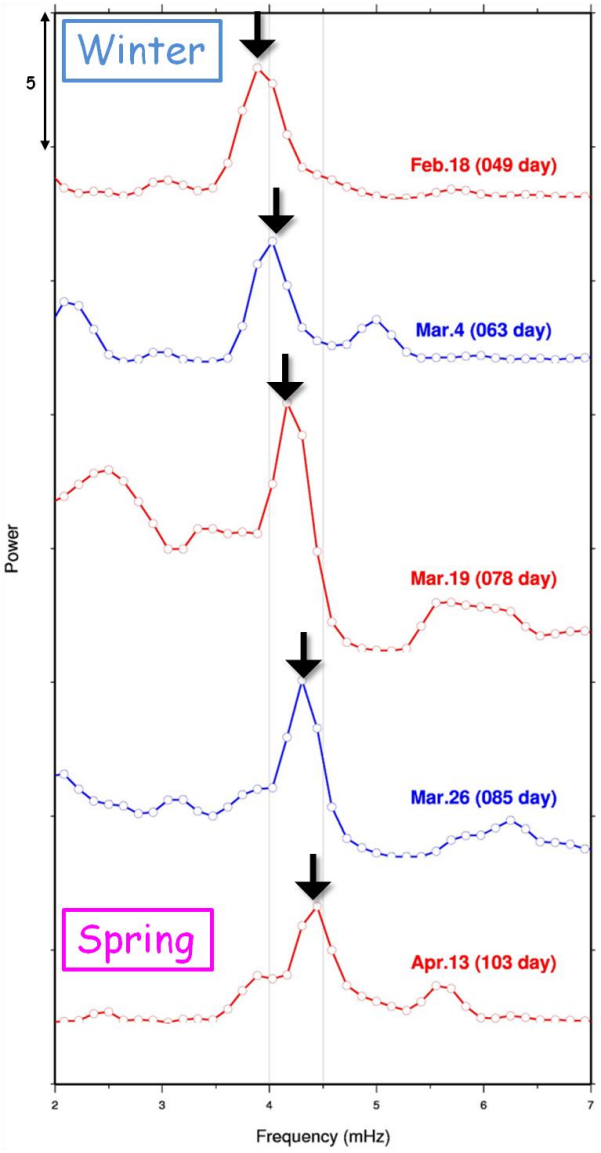

Figure. 2.5 : L4 phase fluctuation spectrogram at the GEONET site 020877 in Shinshinotsu on five different days in 2009, obtained by observing Sat.19. The peak frequency in the February 18 is lower than those in March.

2.2 Conversion from peek frequency to snow depth

After observing L4 phase (TEC) fluctuation time series, their spectrum is analyzed using the Blackman-Tukey method (Hino, 1984). They usually have two frequency peaks corresponding to changes in L1 and L2 phases. In this study, we analyze multipath in L2 because it usually shows a clearer spectral peak than L1. The L2 multipath frequency of a GPS antenna with height of ~5 meters, i.e. a snow-free situation, is ~4.5 mHz (period ~3.7 min). The frequency becomes lower as snow pack develops (as apparent antenna height lowers) in winter, and the L2 multipath frequency decreases by ~0.75 mHz when the snow depth reaches 1 meter (i.e. apparent antenna height is ~4 meter). I calculated the calibration curve to relate multipath frequencies to snow-depth in advance (Fig. 2.6).

This calibration curve has to be changed slightly when we observe different satellite or at a different GPS site (because the changing rate of satellite elevation is different). B the way, the difference of reflectivity at the snow surface alters amplitudes of multipath components, but does not influence the multipath frequencies (Eq. 2.1). Thus I got snow depth time series from daily multipath frequencies.

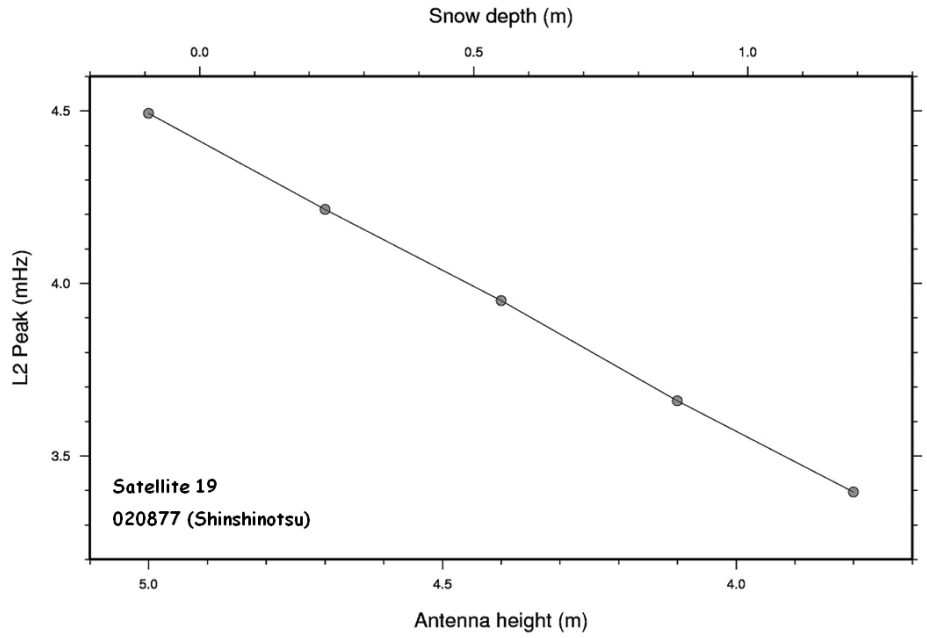

Figure. 2.6 : Relationship between the L2 peak frequency and the snow depth inferred with synthesized data at the GEONET site 020877 in Shinshinotsu, Sat.19. In this case, the calibration equation can be represented by [snow depth (m) = (4.4 – (frequency peak)) / 0.93].

3 Differences from the past study

Temporally changing phase of the reflected wave causes change in amplitude and phase of the total received signal. Larson et al. (2009) measured snow depths by analyzing fluctuations in signal-to-noise ratio (SNR). This corresponds to measure the change in amplitudes of the received signals. On the other hand, we measured snow depths by analyzing fluctuations of phases of L4. Both of them observe changing phases of the received signals using geometry-free observables, but they are completely different in the actually observed quantities.

Larson et al. (2009) tried to recover snow depth time series at the Marshall, Colorado, site (Fig. 3.1) in spring 2009 for two one-week-long periods covering significant snow fall/melt events (Fig. 3.2). Another difference is that we performed data analysis over an entire winter at a more snowy GPS point. Their GPS results showed good agreement with the field measurements, and nearby ultrasonic snow depth sensors (Fig. 3.2). They converted movement of multipath peak frequency in SNR period into snow depth in a similar manner as the present study. I will compare snow depth results by L4 and SNR and discuss benefit and drawbacks of the two methods later in this thesis.

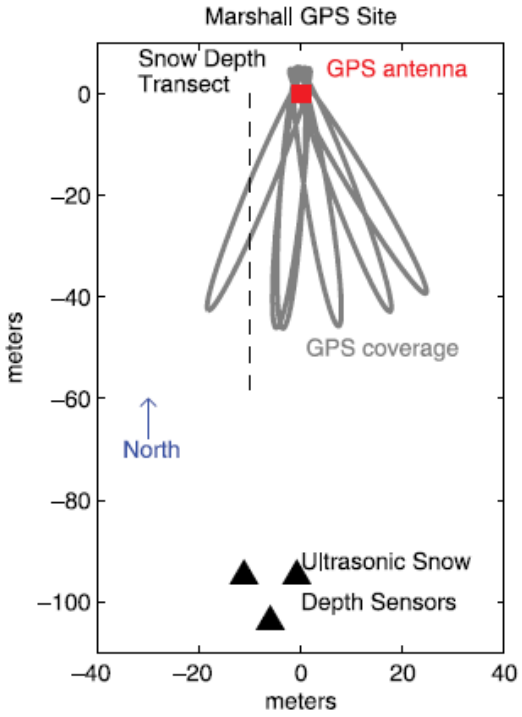

Figure. 3.1 : Map view of the Marshall, olorado site with GPS antenna location (red square), its Fresnel zones at an elevation angle of 5 degrees, and the location of the ultrasonic snow depth sensors (triangles) after Larson et al (2009). The location of the measured snow depth transect is also shown (black dashed line).

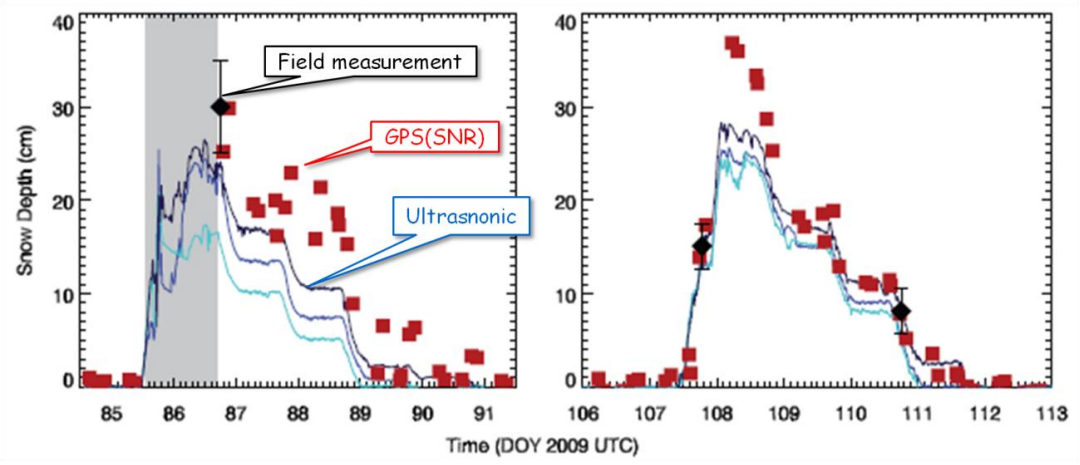

Figure. 3.2 : Snow depth time series derived from GPS (red squares), the three ultrasonic snow depth sensors (blue lines) and field measurements (black diamonds) (Larson et al., 2009).

4 Observing point and period

In this study, I used data at a GEONET (GPS Earth observation Network System) site 020877 in Shinshinotsu, northeast of Sapporo, from January to April in 2009 (Fig. 4.1). During this period, this antenna stood in an open ground, and we could analyze multipath signals of multiple satellites under an ideal condition.

Figure. 4.1 : GPS station at GEONET site 020877 in Shinshinotsu, northeast of Sapporo.

Another benefit of this GPS station is the presence of the AMeDAS (Automatic Meteorological Data Acquisition System) ultrasonic snow depth meter located ~500 m to the west. So this place is suitable for comparing snow depths measured by GPS (L4 and SNR) with those measured by a conventional snow depth meter.
I used data over two hour's period of sat.18, 21, 24 before they sank and sat.16, 18, 19, 29, 31 after they rose (e.g. Fig. 4.3-4, data within green squares). Observing time window was shifted forward four minutes every day, to keep the direction of satellite same.

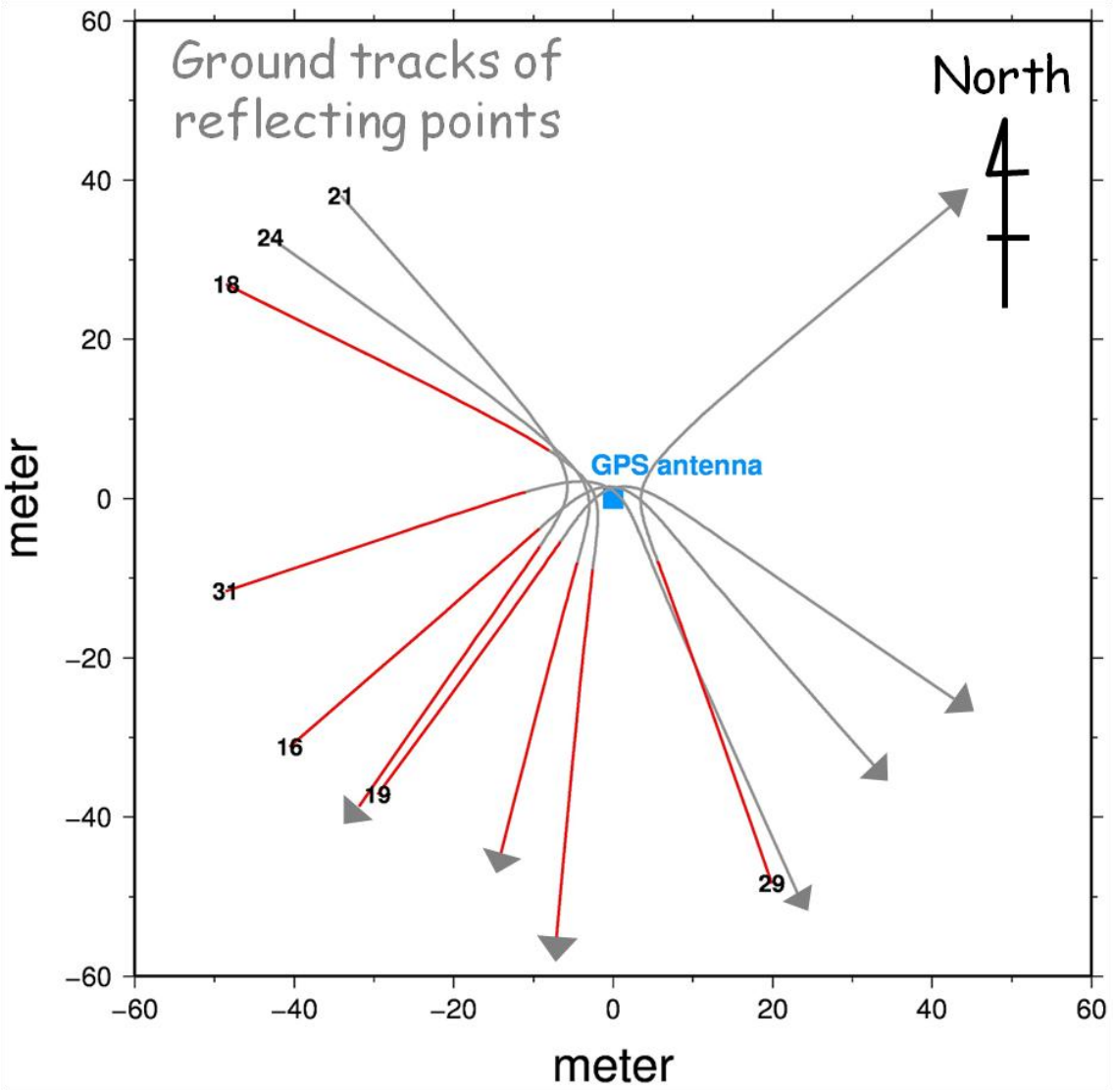

Figure. 4.2 : Shinshinotsu site (GPS antenna at blue square). Gray curves indicate ground tracks of reflecting points of various GPS satellites. GPS satellites move toward the direction of the arrow. I used the red parts to obtain snow depths.

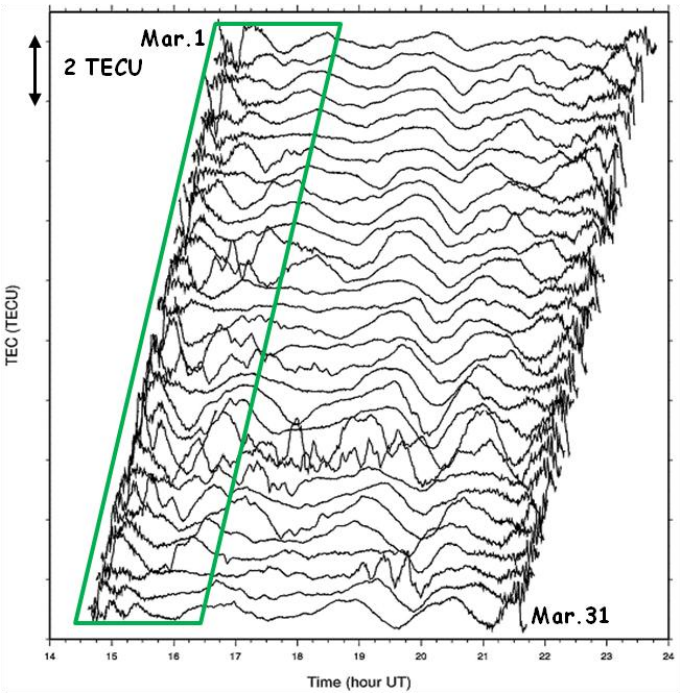

Figure. 4.3 : Time series of L4 in 1-31 March 2009, Sat.19.
The uppermost time series is that on Mar. 1. 2009, and the lowermost time series is that on Mar. 31. 2009.

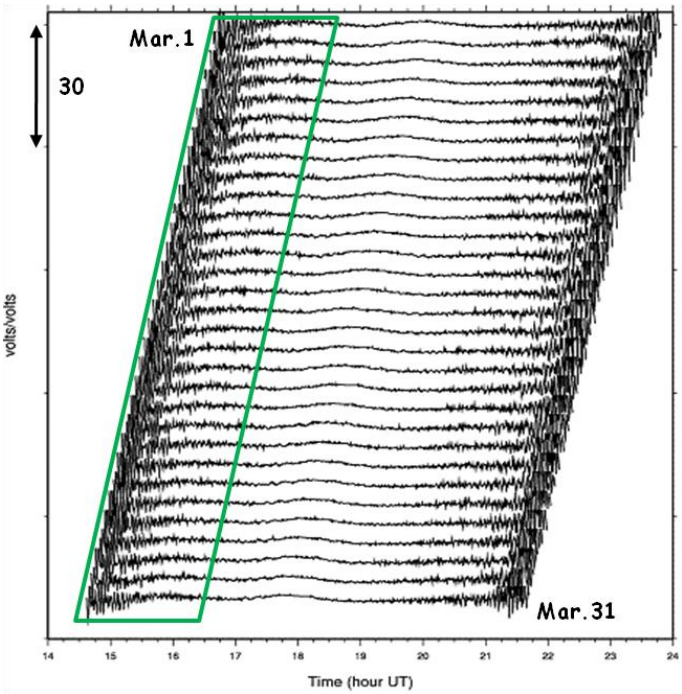

Figure. 4.4 : Time series of SNR (same period, satellite as Fig. 4.3)

5 Results

5.1 Results from single satellites

I first show snow depth results obtained by analyzing L4 and SNR data from one satellite. The following figures (Fig. 5.1-16) show snow depth time series obtained in this way.

Results by L4 (Fig. 5.1-8)

In Fig. 5.1 (top), I show raw time series of daily snow depth measurements obtained analyzing multipath signatures in L4 for satellite 18 over two hour's period before the satellite sinks. The overall trend is similar to the AMeDAS snow depth results, but the data have scatter of a few tens of centimeters. There colors of individual data show strength of multipath peak *1. Data shown with blue colors have lower peaks than those in red. We can see that data showing anomalously large snow depths are all in blue, i.e. they are based on relatively weak peaks. In Fig. 5.1 (bottom), I smoothed the time series by taking running averages over three consecutive days. Now the noise has been significantly reduced.

Similar data processing has been done for seven other satellite's data, i.e. satellite 21 (Fig. 5.2), satellite 24 (Fig. 5.3) over two hour's period before they sink, and satellite 16 (Fig. 5.4), satellite 18 (Fig. 5.5), satellite 19 (Fig. 5.6), satellite 29 (Fig. 5.7), satellite 31 (Fig. 5.8) over two hour's period after they rise. They show similar behaviors to satellite 18 (before sink), but data from satellite 21, 24, 18 (after rise) are less noisy than those with other satellites. This might reflect difference in the snow surface actually measured with these satellites. The reflecting points of GPS satellites (Fig. 4.2) show that the reflecting points of these three data are located southwest of the GPS antenna. I think this ground was stable and unaffected during observing period. Also it is recognized that the snow depth data recovered using GPS data are almost always smaller than the AMeDAS data. This point will be discussed later in detail.

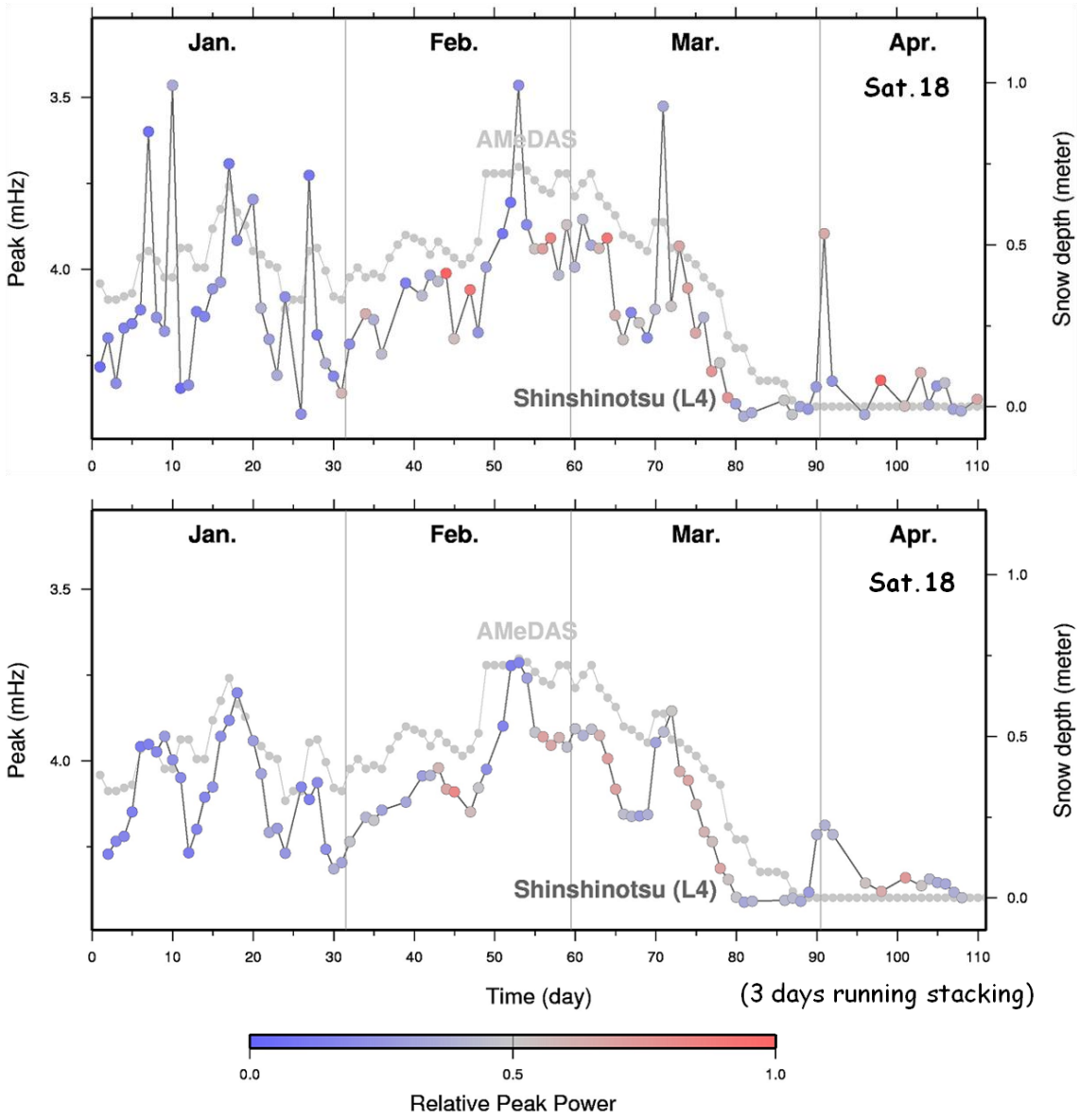

Figure. 5.1 : Raw (above) and 3 days running stacking (bellow) snow depth time series obtained by Sat.18 data before the satellite sinks, and AMeDAS snow depth time series (gray circle). Color scale shows multipath frequency relative peak power.

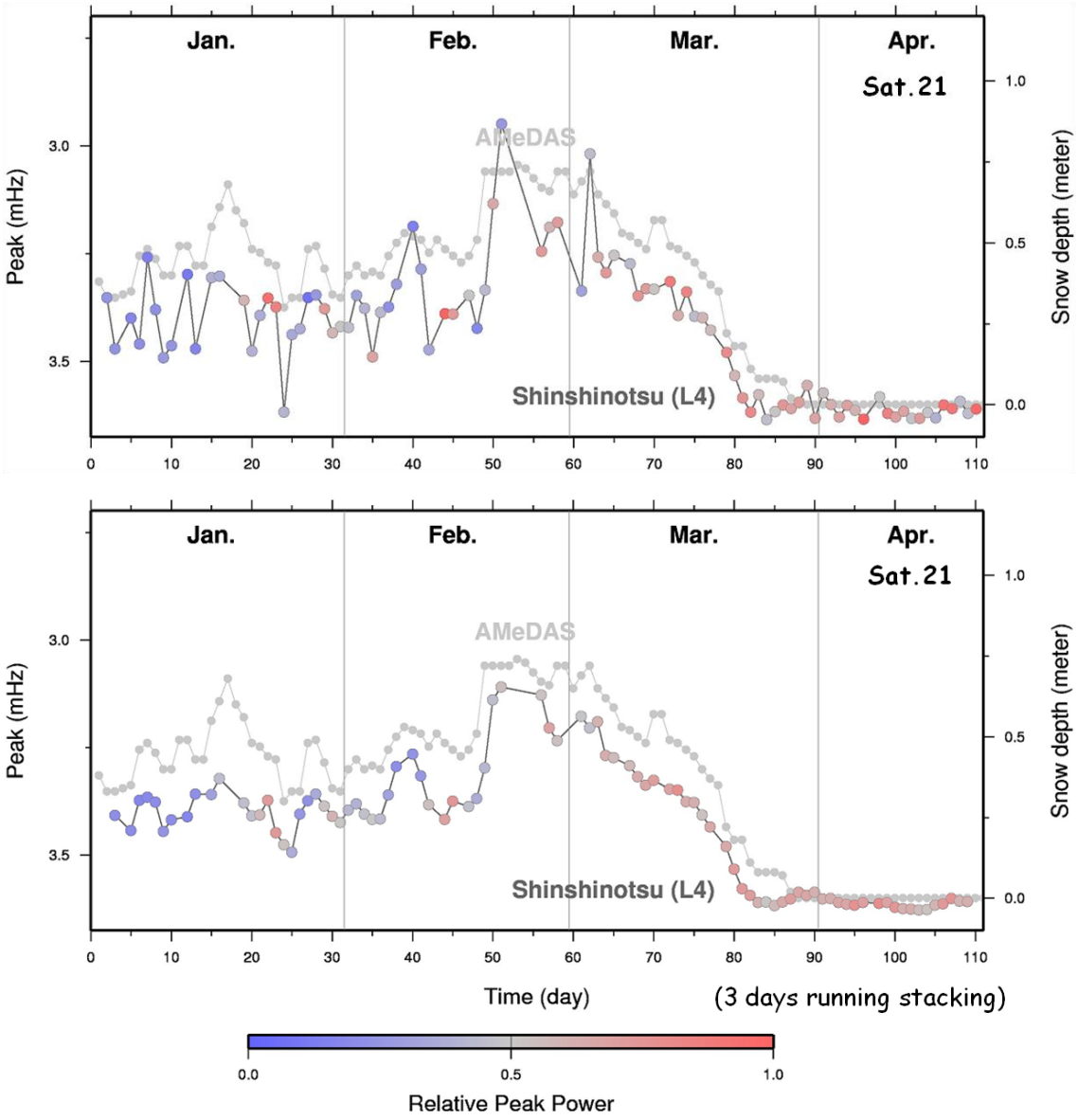

Figure. 5.2 : Raw (above) and 3 days running stacking (bellow) snow depth time series obtained by Sat.21 data before the satellite sinks, and AMeDAS snow depth time series (gray circle). Color scale shows multipath frequency relative peak power.

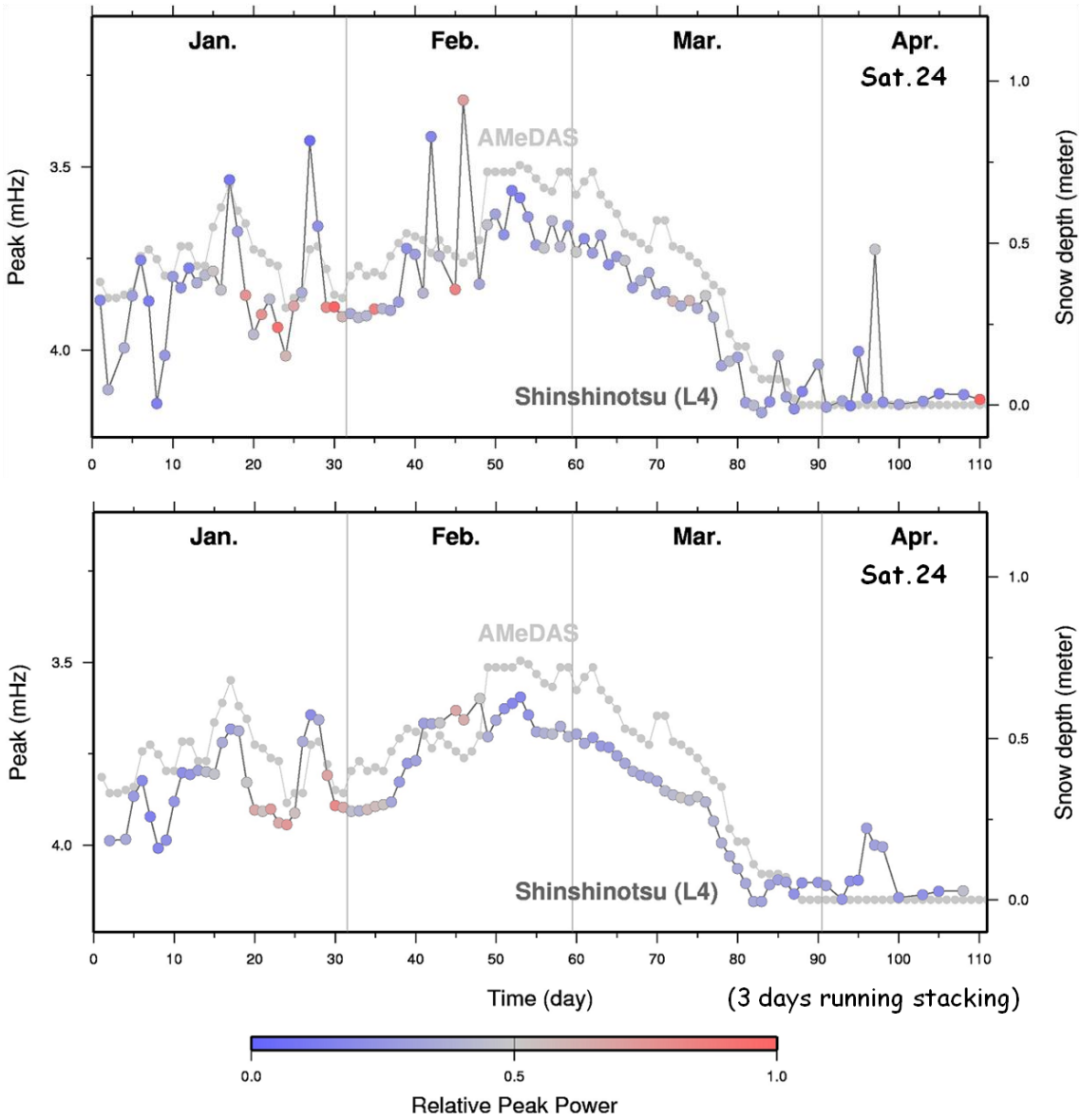

Figure. 5.3 : Raw (above) and 3 days running stacking (bellow) snow depth time series obtained by Sat.24 data before the satellite sinks, and AMeDAS snow depth time series (gray circle). Color scale shows multipath frequency relative peak power.

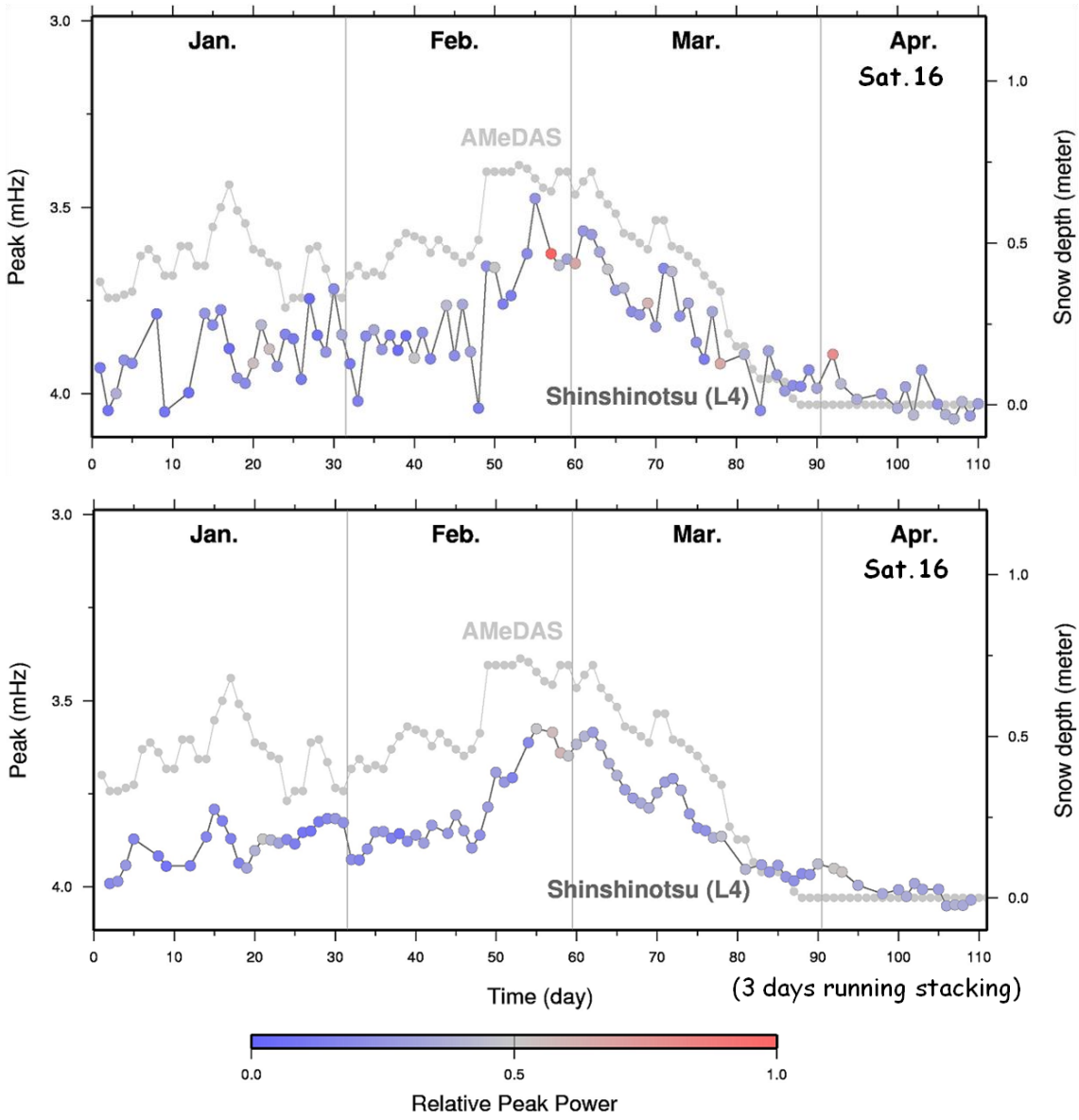

Figure. 5.4 : Raw (above) and 3 days running stacking (bellow) snow depth time series obtained by Sat.16 data after the satellite rises, and AMeDAS snow depth time series (gray circle). Color scale shows multipath frequency relative peak power.

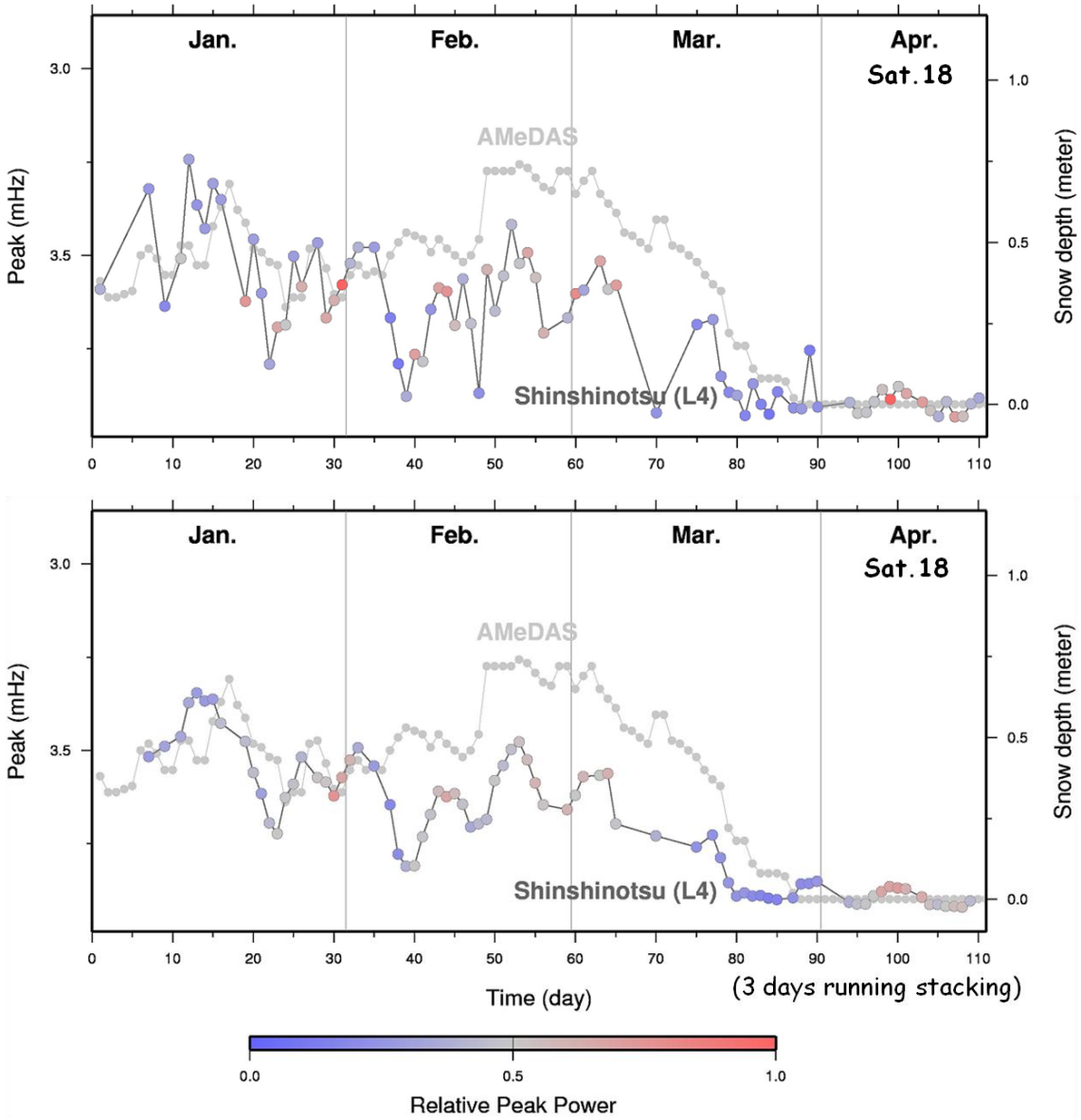

Figure. 5.5 : Raw (above) and 3 days running stacking (bellow) snow depth time series obtained by Sat.18 data after the satellite rises, and AMeDAS snow depth time series (gray circle). Color scale shows multipath frequency relative peak power.

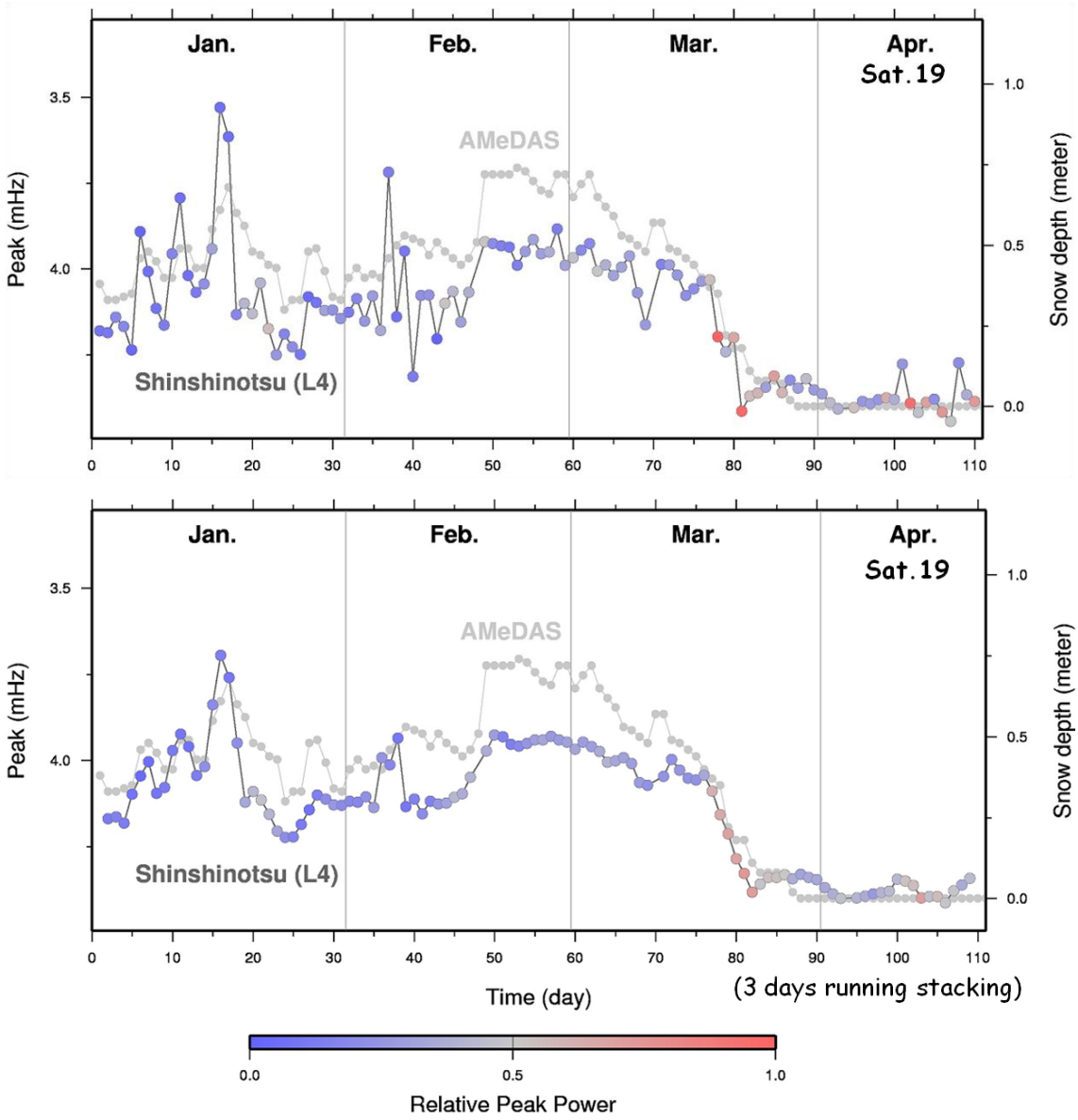

Figure. 5.6 : Raw (above) and 3 days running stacking (bellow) snow depth time series obtained by Sat.19 data after the satellite rises, and AMeDAS snow depth time series (gray circle). Color scale shows multipath frequency relative peak power.

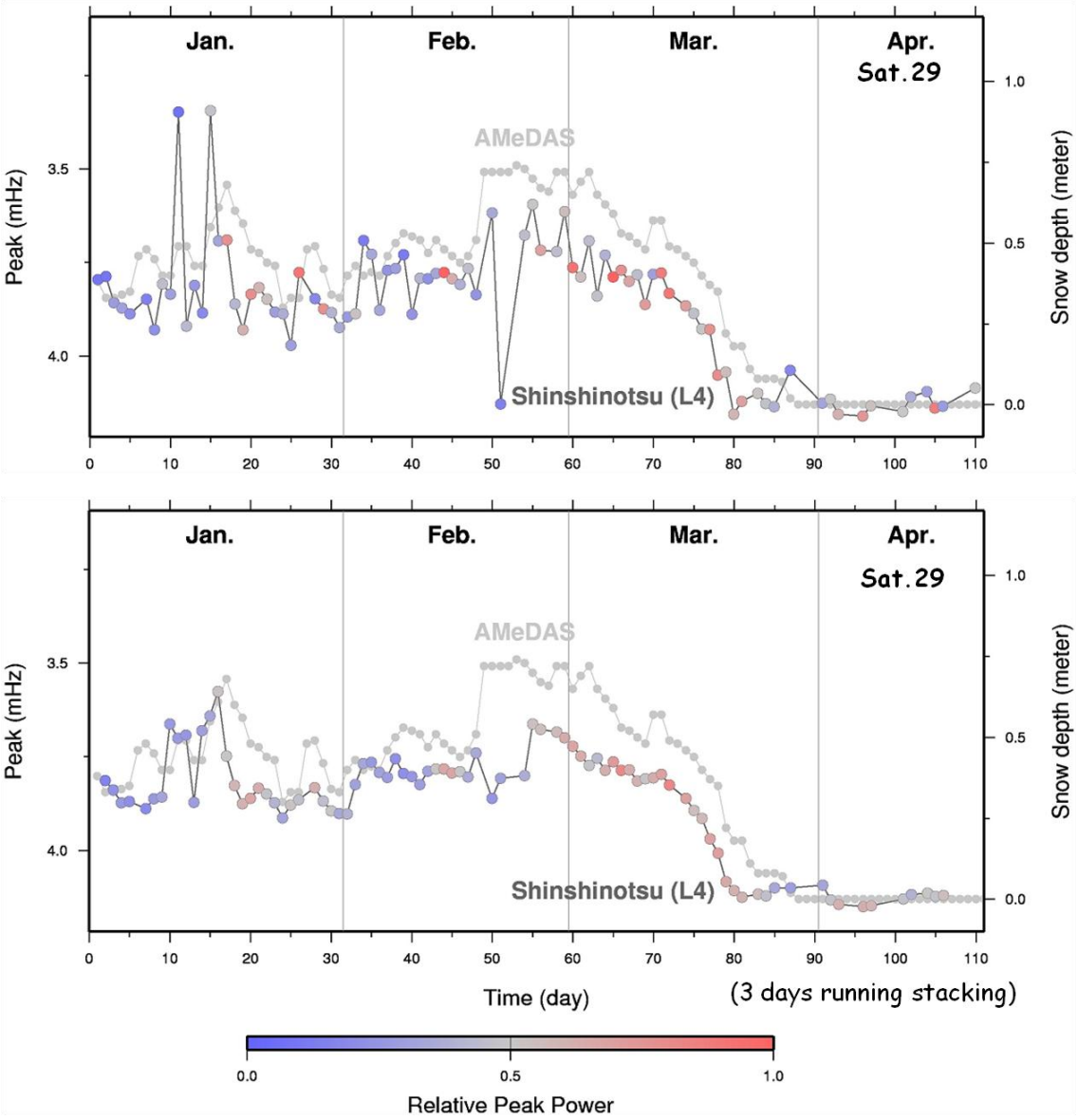

Figure. 5.7 : Raw (above) and 3 days running stacking (bellow) snow depth time series obtained by Sat.29 data after the satellite rises, and AMeDAS snow depth time series (gray circle). Color scale shows multipath frequency relative peak power.

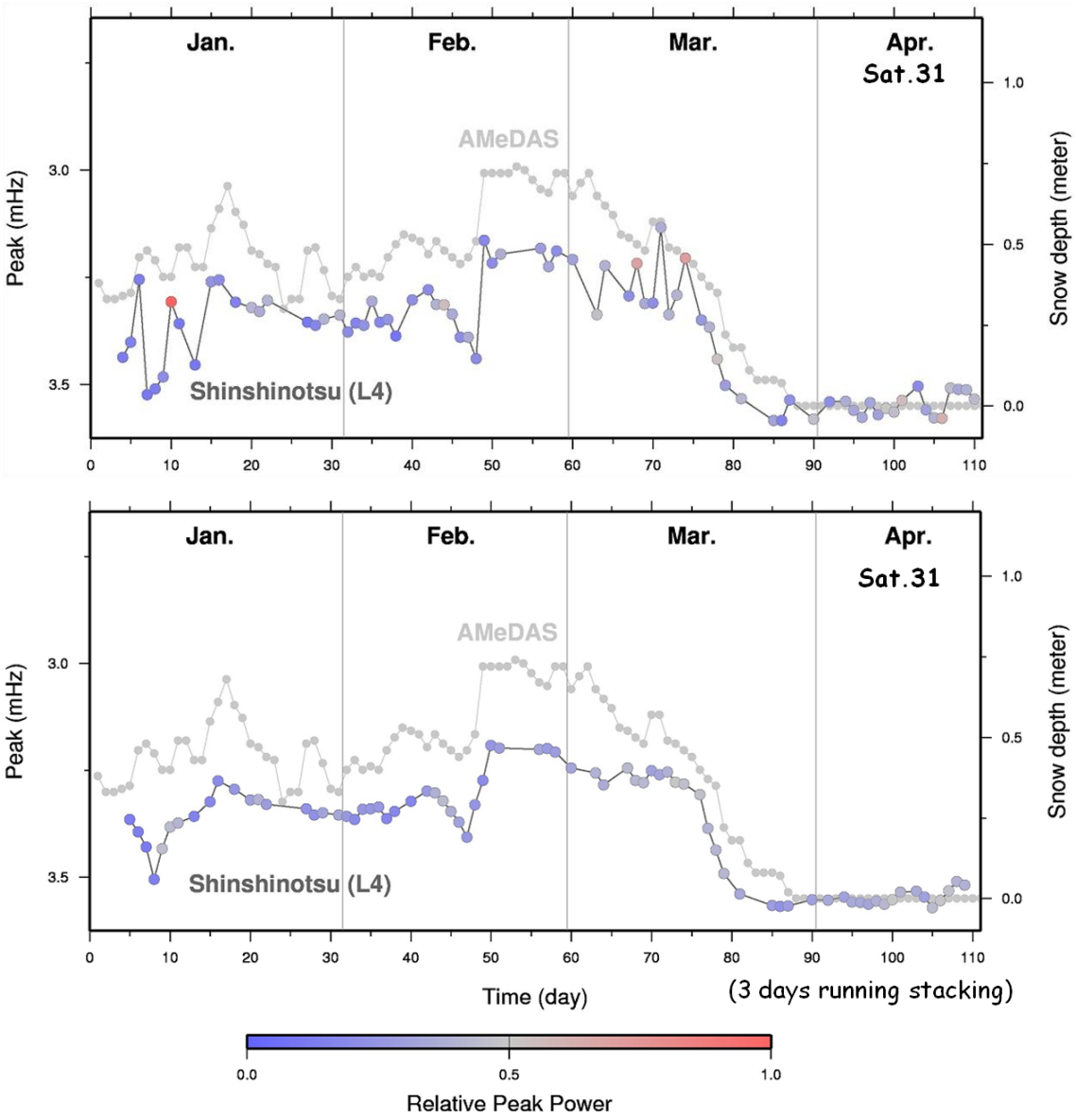

Figure. 5.8 : Raw (above) and 3 days running stacking (bellow) snow depth time series obtained by Sat.31 data after the satellite rises, and AMeDAS snow depth time series (gray circle). Color scale shows multipath frequency relative peak power.

Results of SNR (Fig. 5.9-16)

Data processing similar to L4 has been done for the same eight satellite's using SNR data, i.e. satellite 18 (Fig. 5.9), satellite 21 (Fig. 5.10), satellite 24 (Fig. 5.11) over two hour's period before they sink, and satellite 16 (Fig. 5.12), satellite 18 (Fig. 5.13), satellite 19 (Fig. 5.14), satellite 29 (Fig. 5.15), satellite 31 (Fig. 5.16) over two hour's period after they rise.

They show similar behaviors to L4 data. However, as a whole, SNR data are less noisy than L4 data. One possibility is that good L4 data can be obtained only when phases of reflected microwaves of both L1 and L2 are well observed. In contrast, SNR data can be obtained by observing only either one of the phases. It is also true for both L4 and SNR results that snow depths estimated using satellites 21, 24, 18 (before they sink) and 19 (after it rises) are less noisy than those with other satellites. The reflecting points of these GPS satellites are all located SSW of the antenna. The snow surface in this part might have been more stable and smooth (i.e. less disturbed) during the observing period.

The SNR results also showed the same tendency as L4 results that the snow depths recovered using GPS data are almost always smaller than the AMeDAS data.

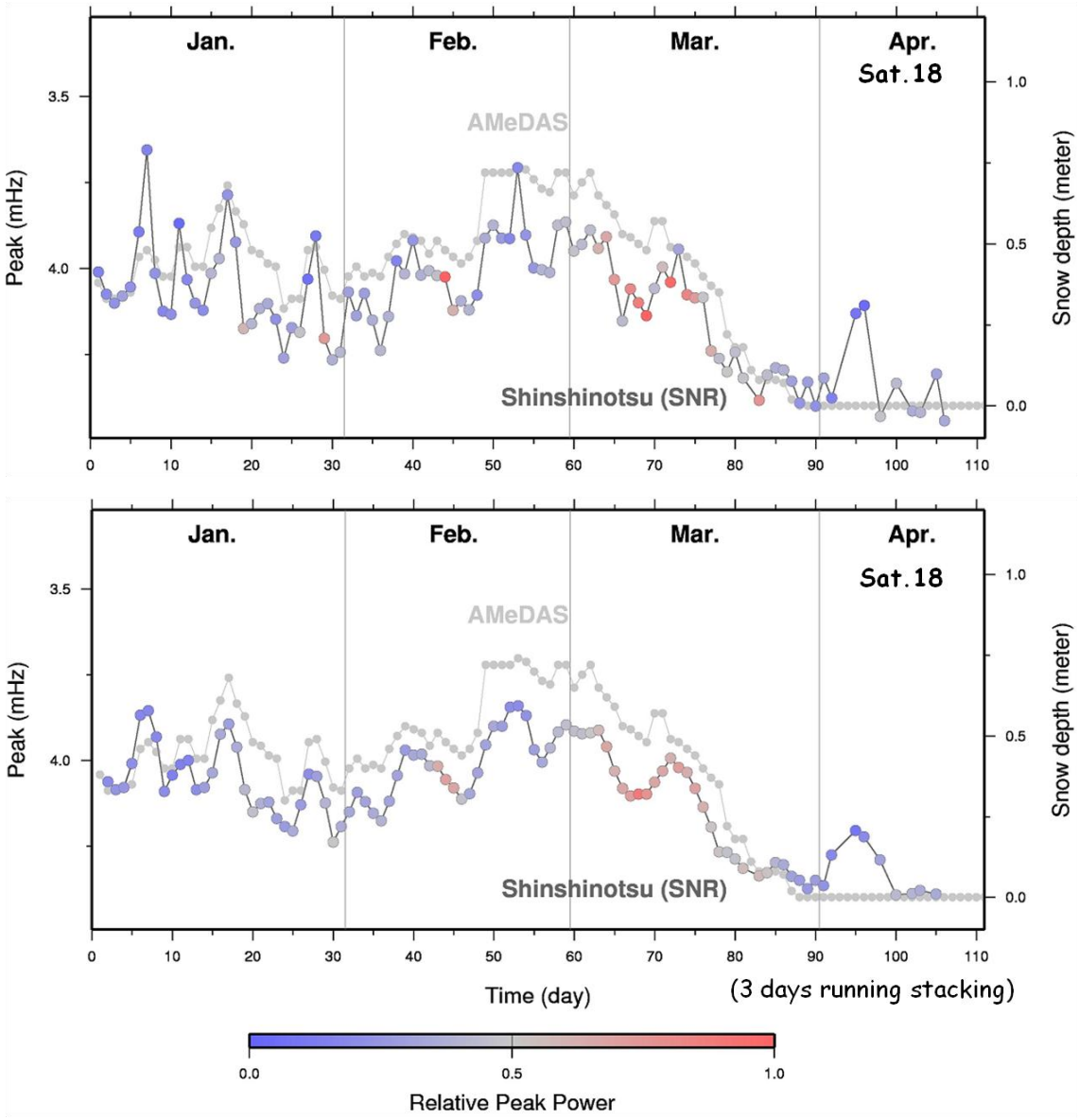

Figure. 5.9 : Raw (above) and 3 days running stacking (bellow) snow depth time series obtained by Sat.18 data before the satellite sinks, and AMeDAS snow depth time series (gray circle). Color scale shows multipath frequency relative peak power.

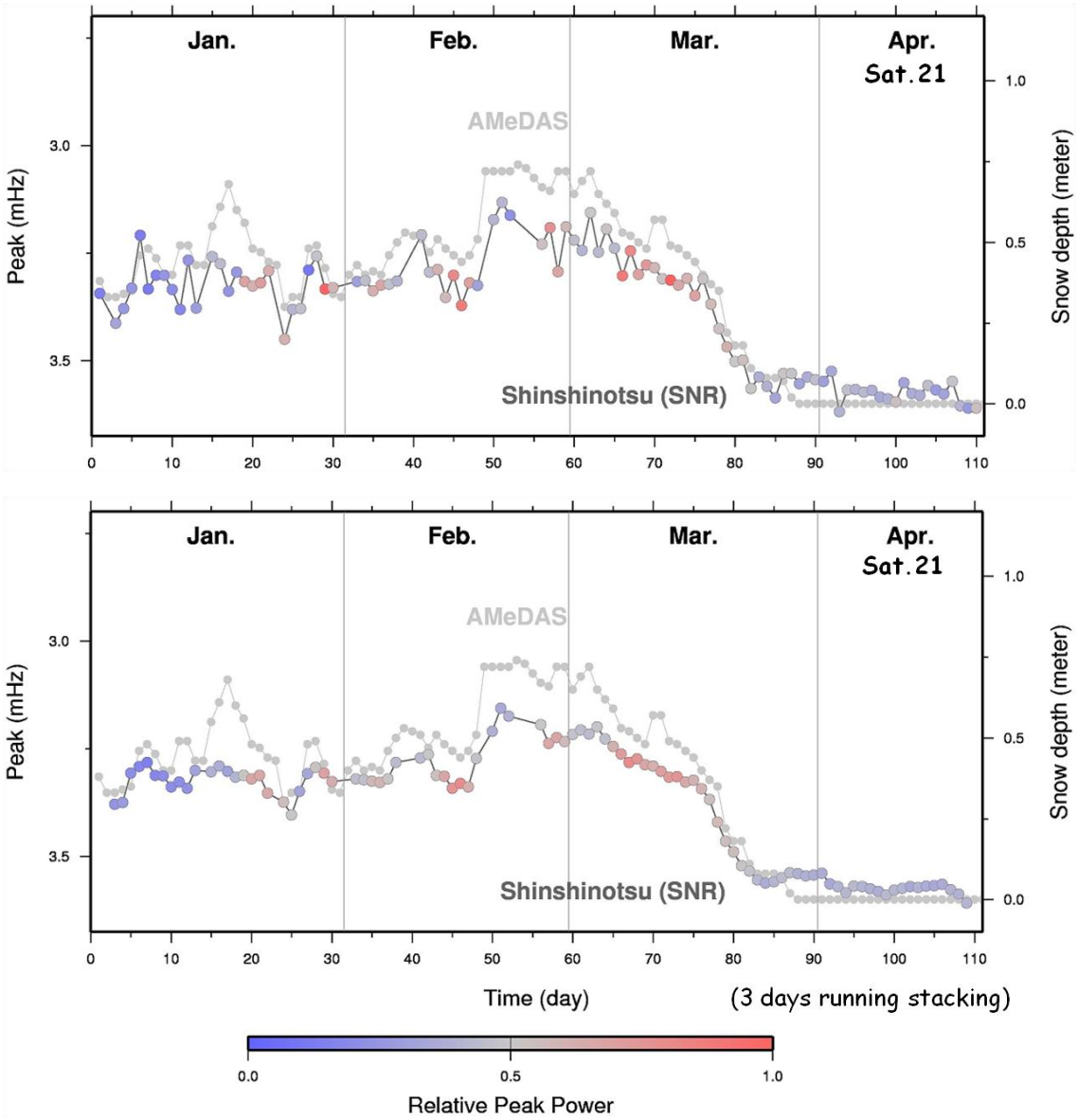

Figure. 5.10 : Raw (above) and 3 days running stacking (bellow) snow depth time series obtained by Sat.21 data before the satellite sinks, and AMeDAS snow depth time series (gray circle). Color scale shows multipath frequency relative peak power.

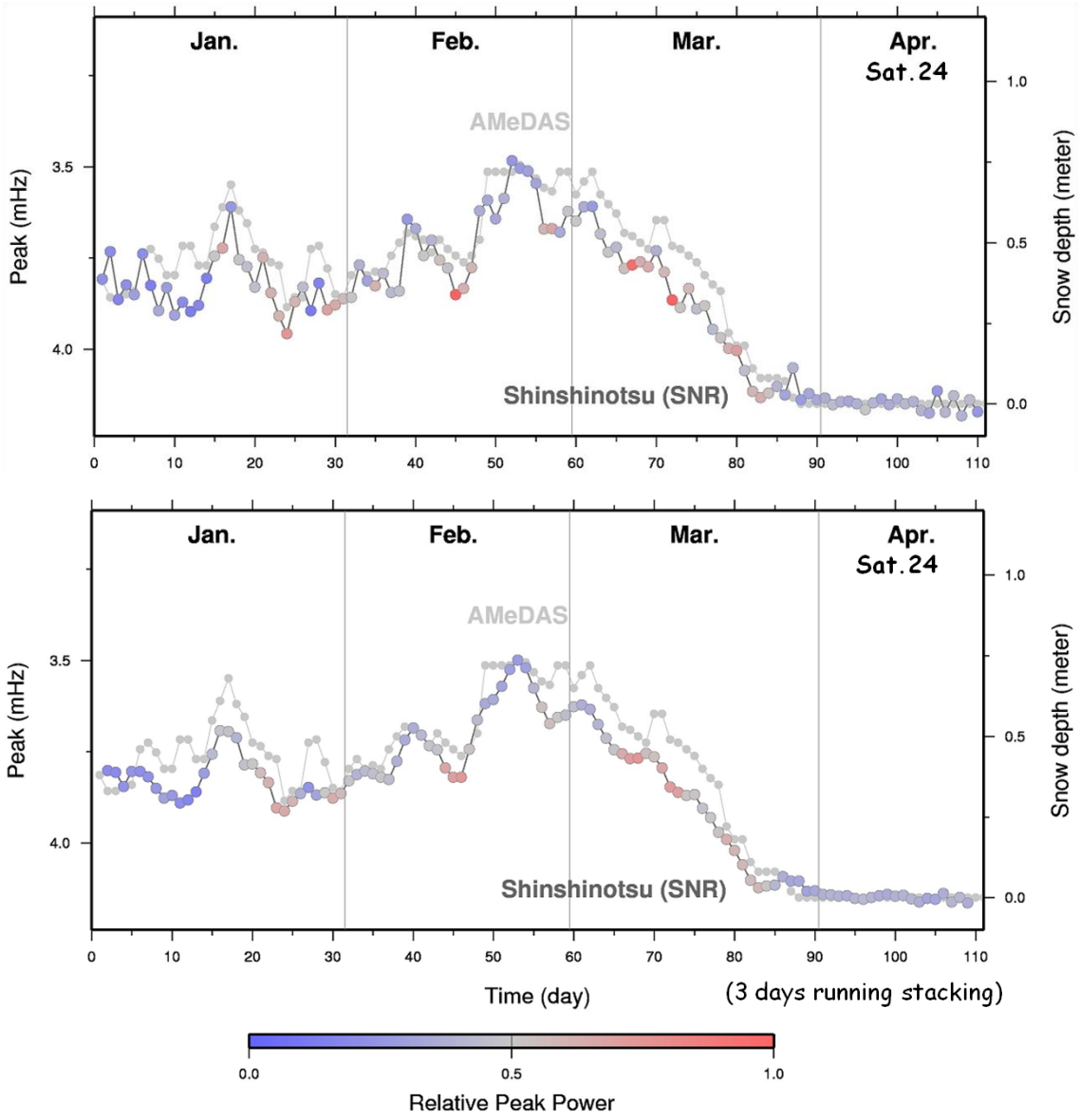

Figure. 5.11 : Raw (above) and 3 days running stacking (bellow) snow depth time series obtained by Sat.24 data before the satellite sinks, and AMeDAS snow depth time series (gray circle). Color scale shows multipath frequency relative peak power.

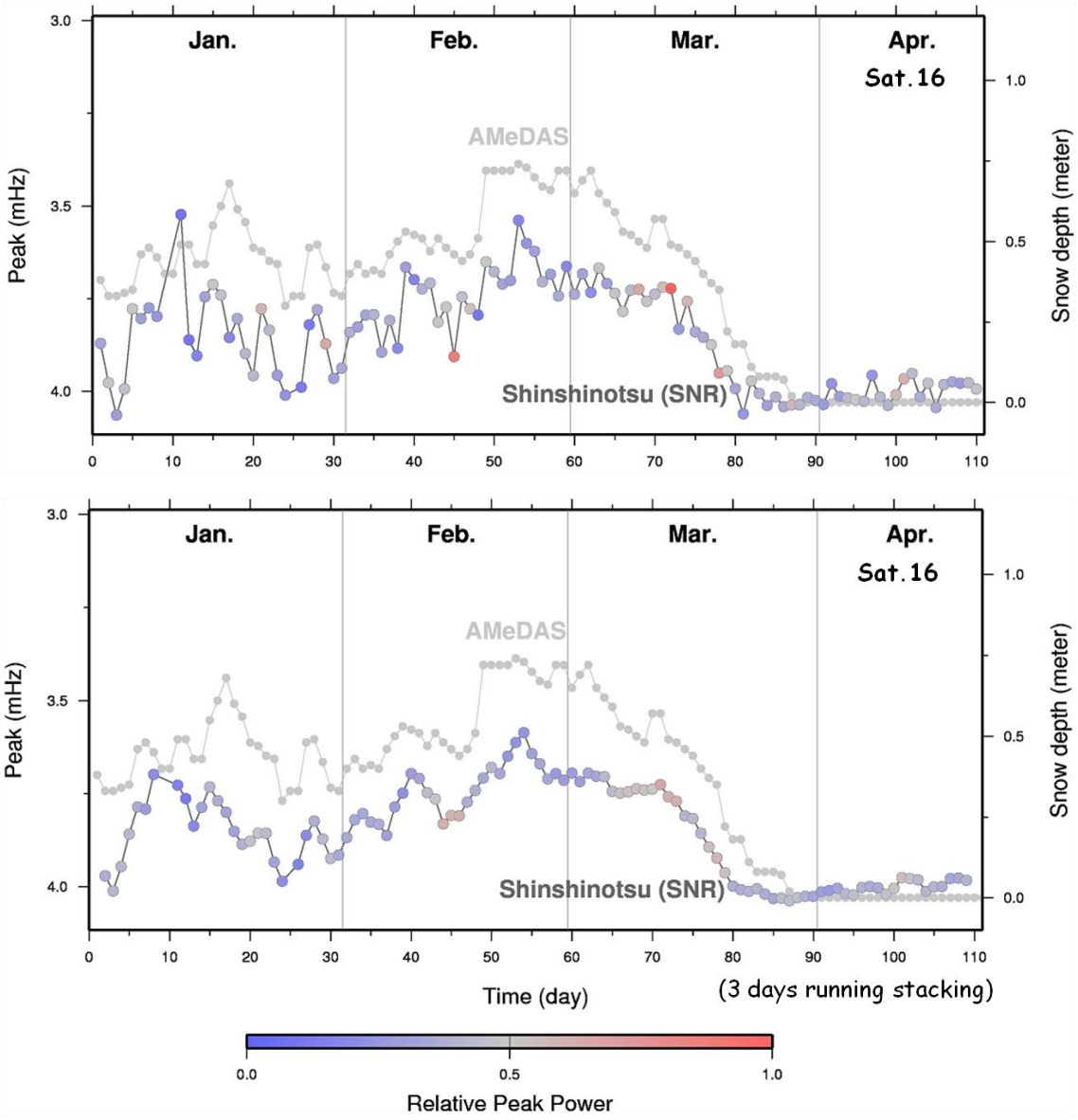

Figure. 5.12 : Raw (above) and 3 days running stacking (bellow) snow depth time series obtained by Sat.16 data after the satellite rises, and AMeDAS snow depth time series (gray circle). Color scale shows multipath frequency relative peak power.

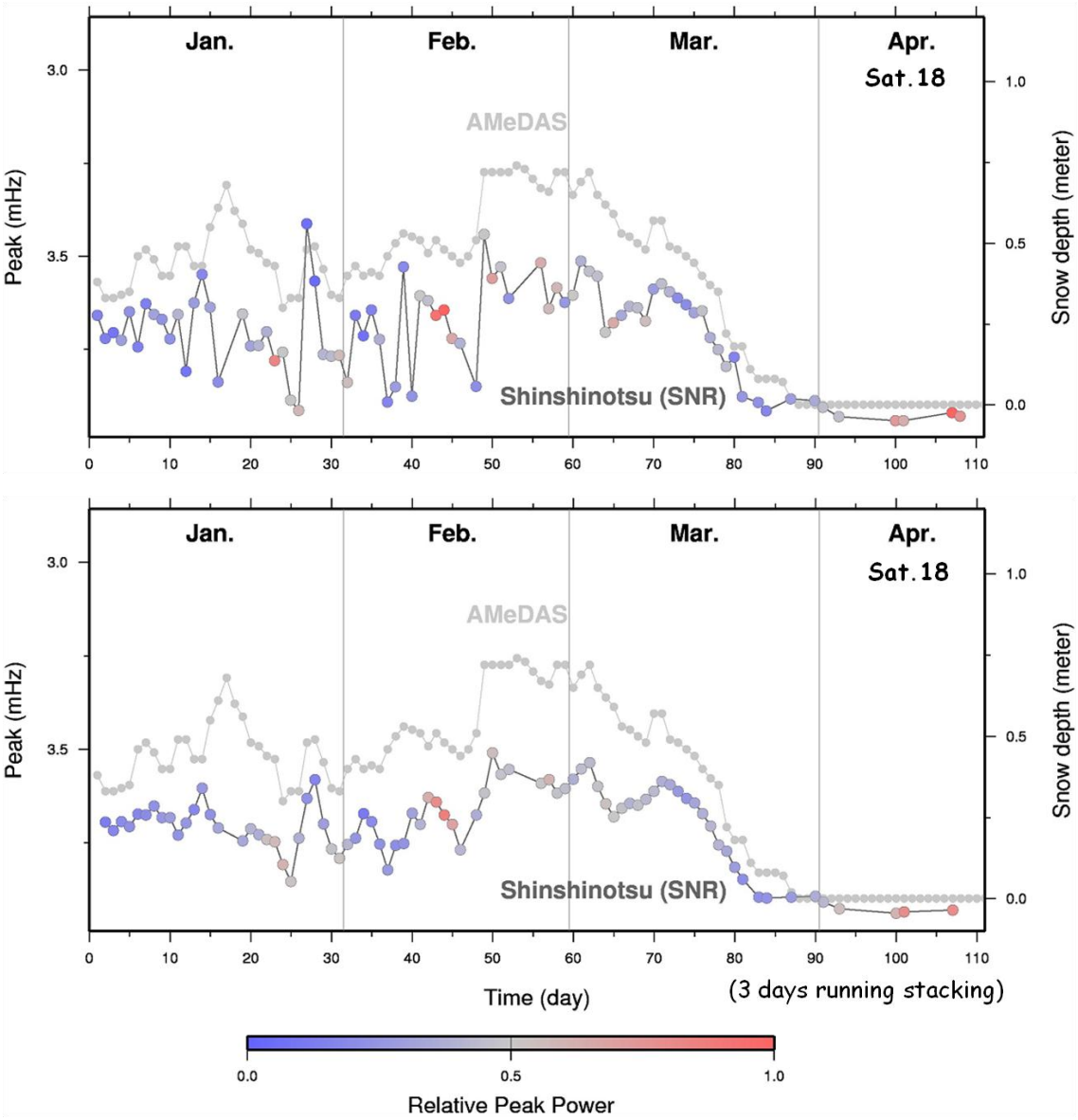

Figure. 5.13 : Raw (above) and 3 days running stacking (bellow) snow depth time series obtained by Sat.18 data after the satellite rises, and AMeDAS snow depth time series (gray circle). Color scale shows multipath frequency relative peak power.

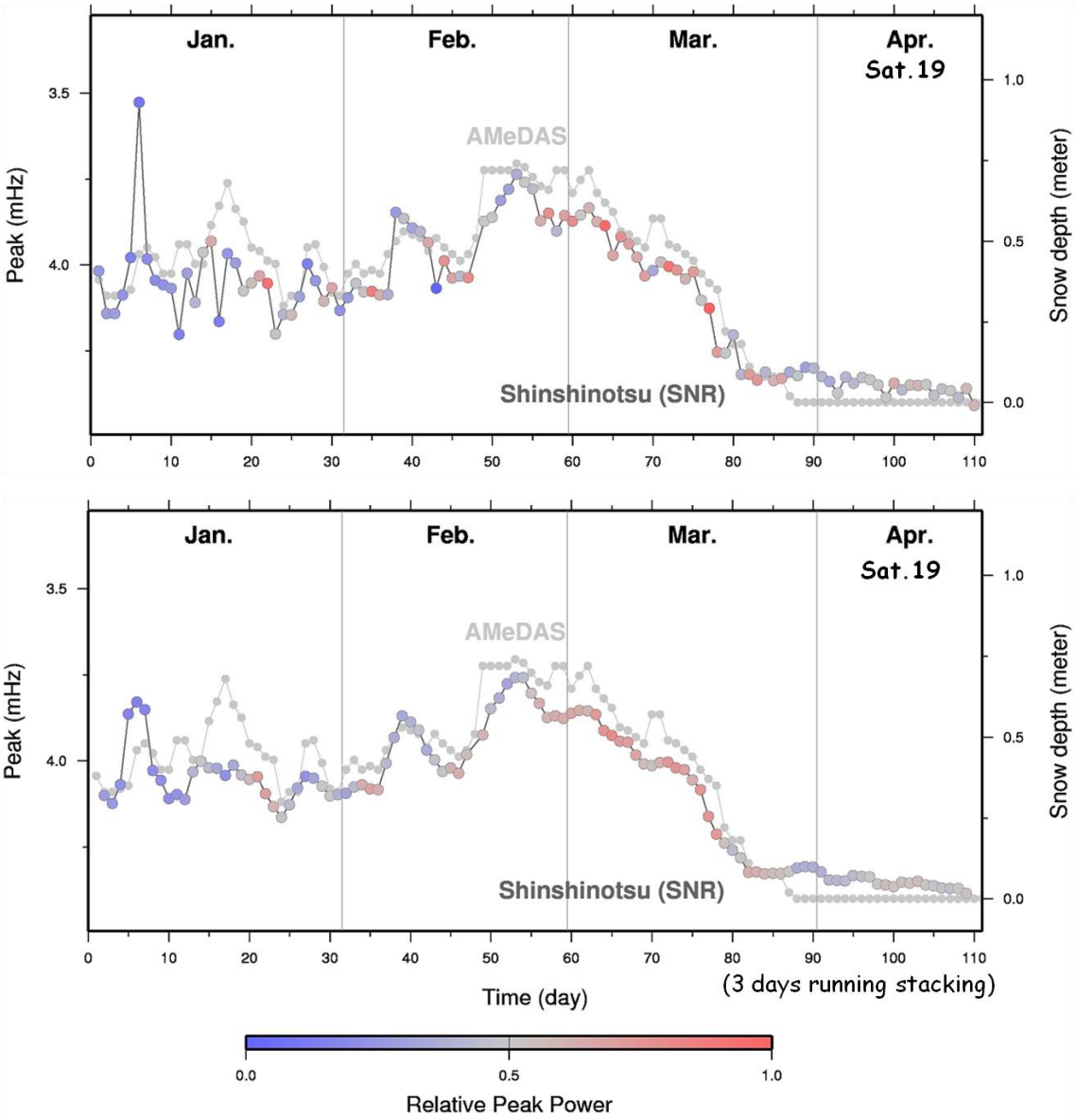

Figure. 5.14 : Raw (above) and 3 days running stacking (below) snow depth time series obtained by Sat.19 data after the satellite rises, and AMeDAS snow depth time series (gray circle). Color scale shows multipath frequency relative peak power.

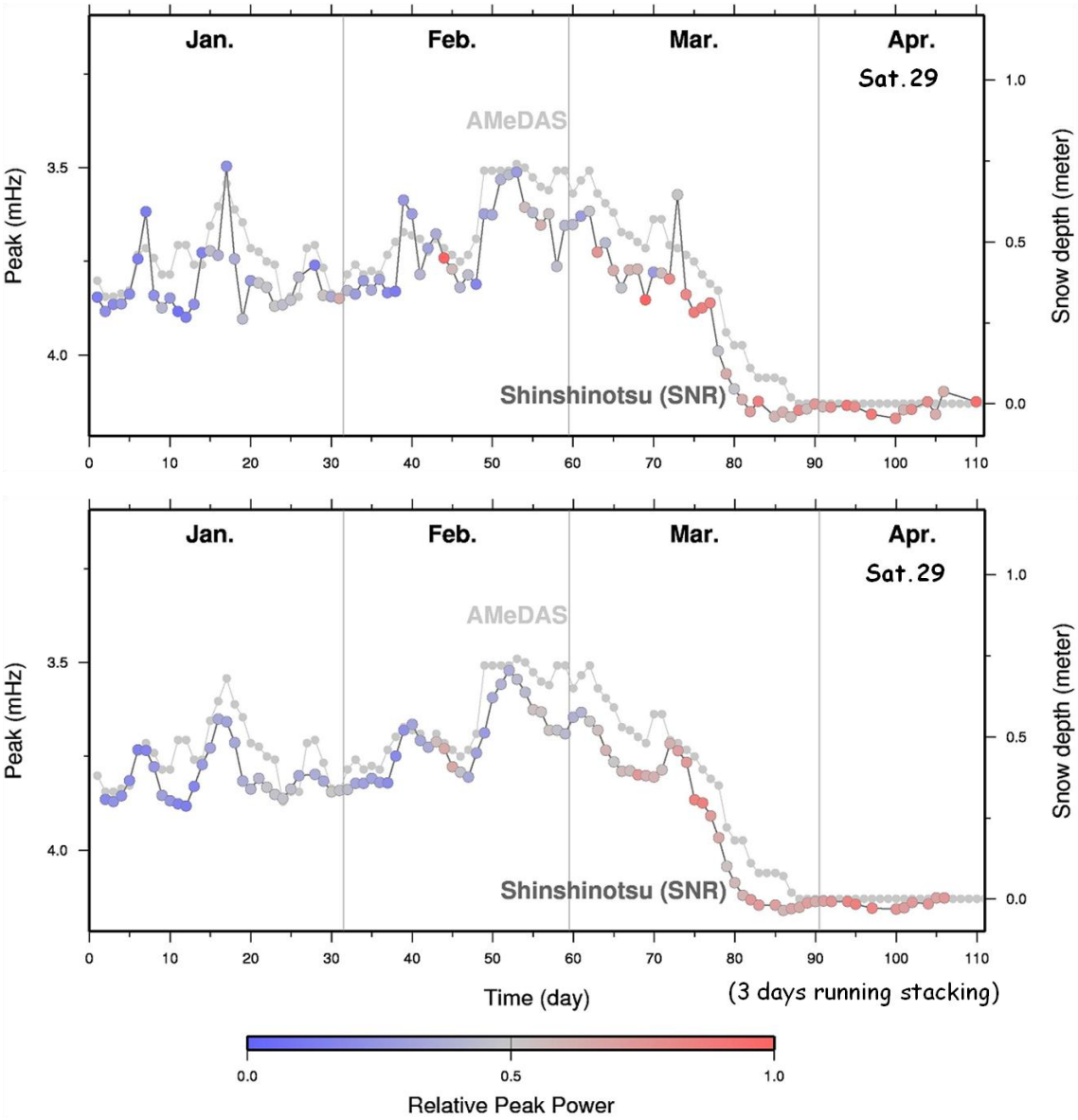

Figure. 5.15 : Raw (above) and 3 days running stacking (bellow) snow depth time series obtained by Sat.29 data after the satellite rises, and AMeDAS snow depth time series (gray circle). Color scale shows multipath frequency relative peak power.

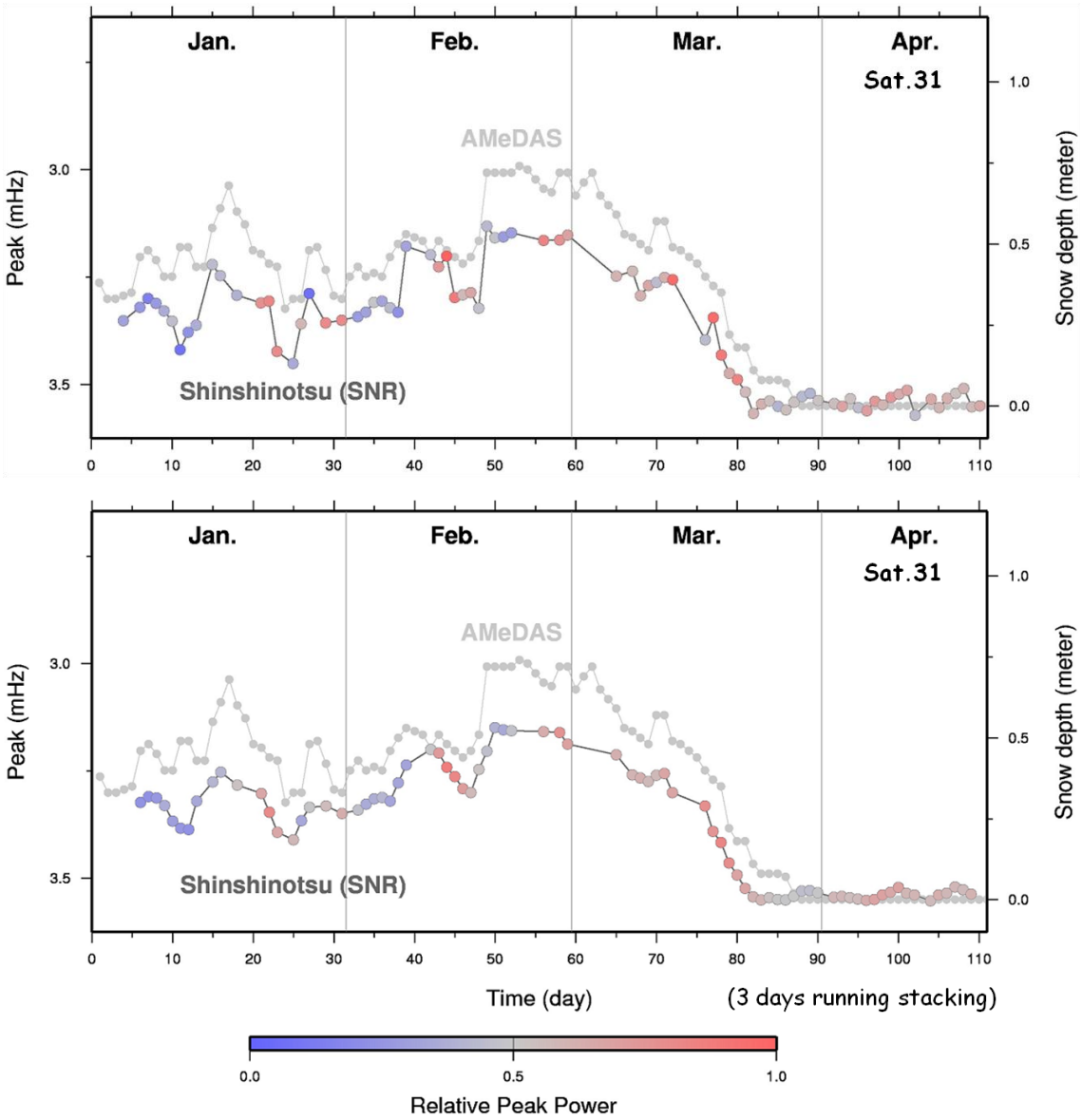

Figure. 5.16 : Raw (above) and 3 days running stacking (below) snow depth time series obtained by Sat.31 data after the satellite rises, and AMeDAS snow depth time series (gray circle). Color scale shows multipath frequency relative peak power.

5.2 Results from multiple satellites

Next I show daily snow depth time series obtained as averages of snow depths estimated with all the available satellites for L4 (Fig. 5.17 top) and SNR (Fig. 5.18 top). In calculating the average, we applied larger weight for data with a higher peak power. Such averaging is equivalent to making the average of snow depths in a large area around the antenna (region within a circle with diameter of ~100 m). This spatial averaging reduced the noise significantly. In Fig. 5.17 (bottom) and Fig.5.18 (bottom), I further performed temporal smoothing by taking running averages over three consecutive days. Now the data showed fairly small noises.

Also, the snow depth data recovered using GPS data tend to underestimate the true depth shown by AMeDAS by a few tens of centimeters.

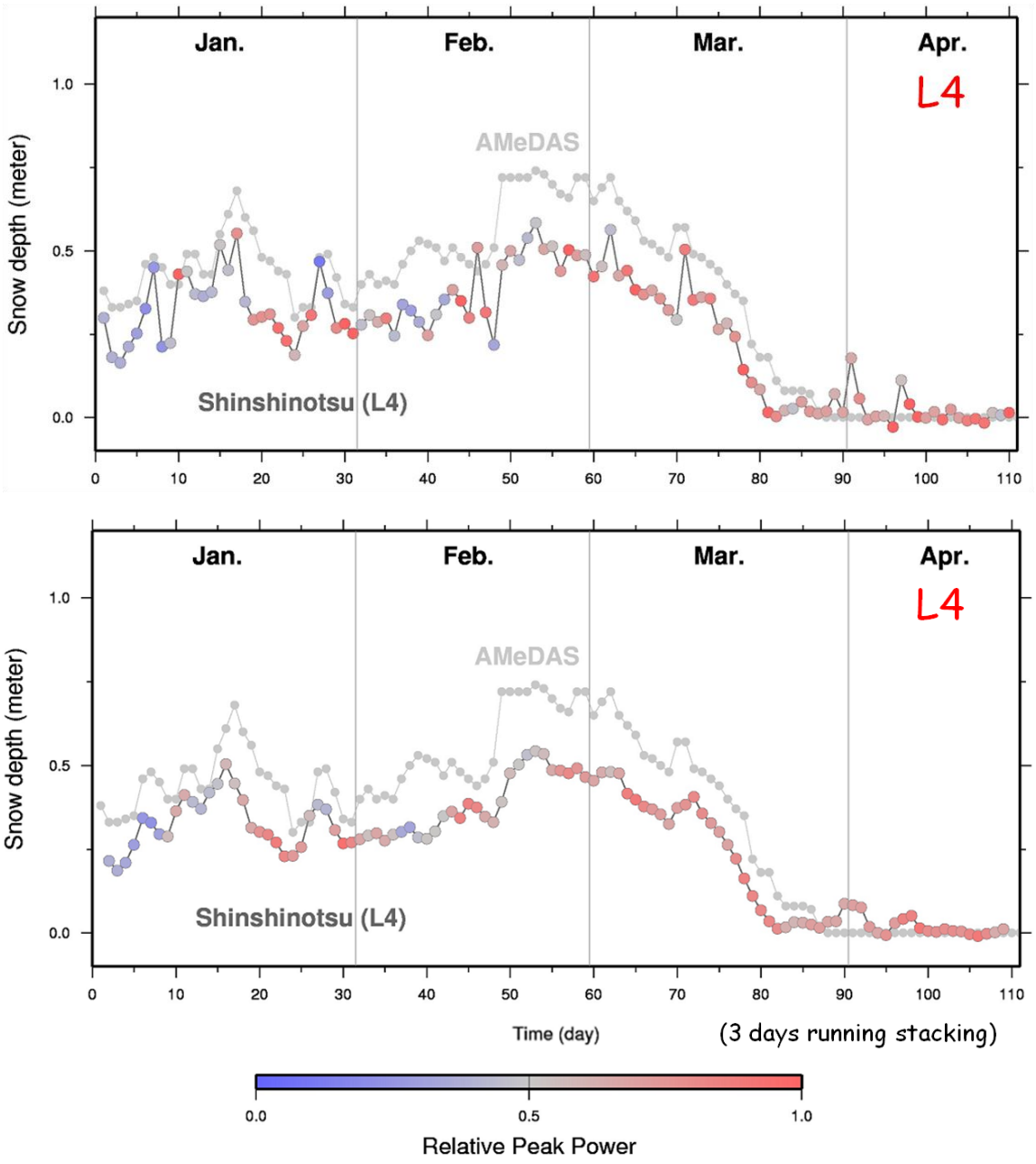

Figure. 5.17 : Snow depth time series obtained as averages of snow depth results inferred by analyzing L4 data from individual satellites. The top and the bottom panels show the raw data and 3 days running averages, respectively. AMeDAS snow depth time series are shown with gray circles. Color scale shows multipath frequency relative peak power.

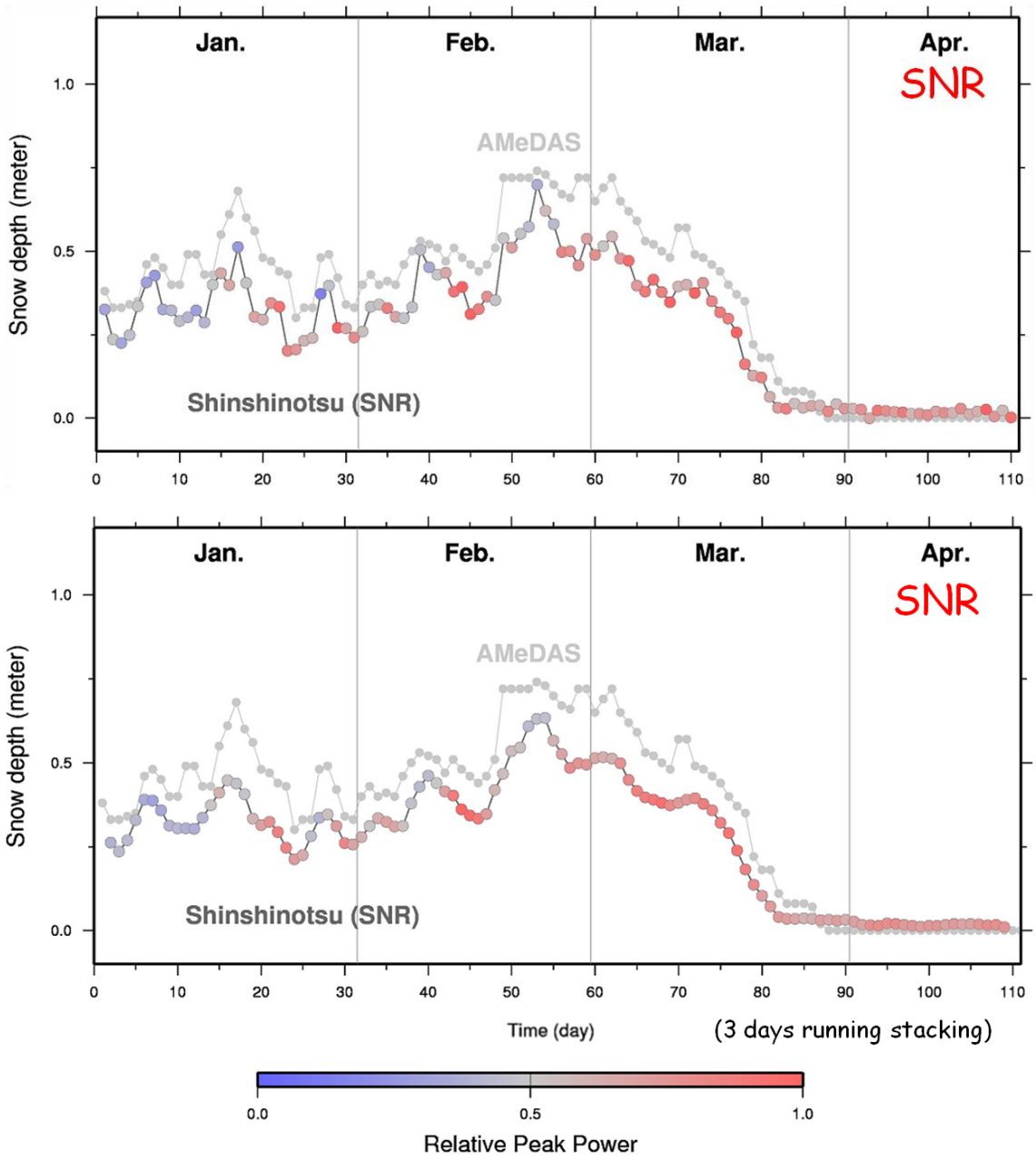

Figure. 5.18 : Snow depth time series obtained as averages of snow depth results inferred by analyzing SNR data from individual satellites. The top and the bottom panels show the raw data and 3 days running averages, respectively. AMeDAS snow depth time series are shown with gray circles. Color scale shows multipath frequency relative peak power.

*1 Description of 'color symbols of snow depths obtained GPS'

The color of the symbols shows the strength of the frequency peak power of the day. For example, Fig. 5.19 shows snow depth time series obtained from sat.19 (top), and three spectrograms (bottom) of the multipath frequency peak on three different days in the time series. The stronger the peak power of the day, the redder the symbol color becomes. For example, the symbol of Mar. 19 has a vivid red color. On this day, the inferred snow depth has a high reliability because multipath signature is captured very clearly. On the other hand, the symbol of Jan.21 has a blue color. On this day, I used the peak whose power is the largest in the search window, but it may not represent the proper multipath signature. When I show the time series of average snow depths of multiple satellites (e.g. Fig. 5.17, 18), the color symbol of that day reflects the strongest peak power within the three days used for averaging.

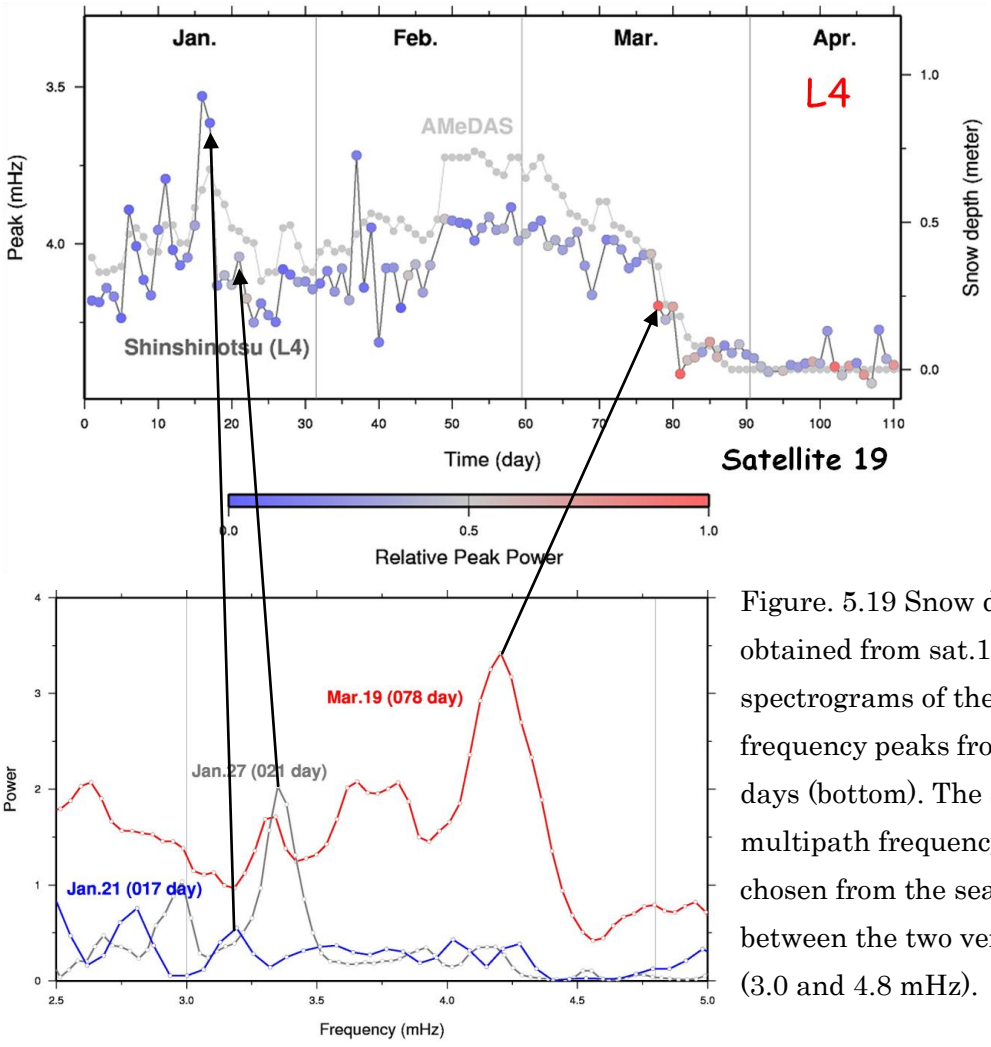

Figure. 5.19 Snow depth time series obtained from sat.19 (top), and spectrograms of the multipath frequency peaks from three different days (bottom). The strongest multipath frequency peaks are chosen from the search window between the two vertical gray lines (3.0 and 4.8 mHz).

5.3 Correction for volume scattering

The snow depth time series results (Fig. 5.17, 18) show that snow depths obtained by GPS (L4 and SNR) are about 10-20 cm lower than those obtained by AMeDAS. It is speculated that this underestimates of snow depths are caused by "volume scattering" of microwave reflected at the snow surface. Microwave may penetrate snow (up to ~50 cm *2) and diffuse within the snow, which is called volume scattering. Diffused microwave partly go to the antenna being mixed with the waves reflected at the snow surface as a specular body. This causes slight increase of the excess path length, and the underestimation of snow depths.

Here I propose a simple method to correct this influence by using frequency peak powers. When snow at the surface is wet and dense (e.g. those in early spring), most of the reflection would be specular. In such a case, the peak of the multipath signature would be clear (peak in the spectrogram would be strong). On the other hand, freshly fallen snow in middle winter would be light (porous) and larger volume scattering would occur. In such a case, the multipath signature would be ambiguous (weak peak). Hence, the snow depth of a day with lower frequency peak power would need larger correction because of larger amount of volume scattering (Fig. 5.20).

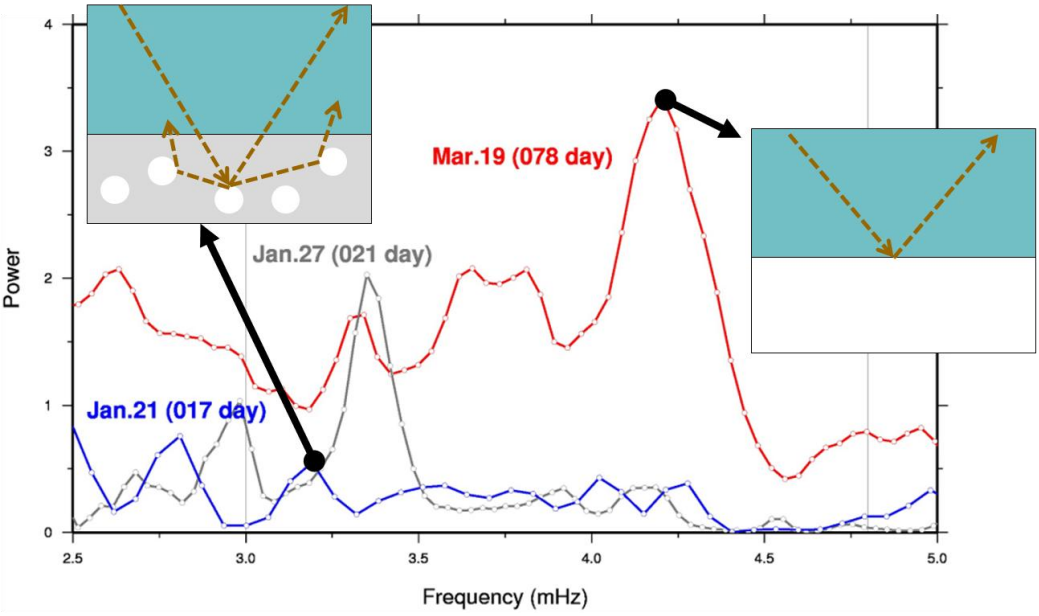

Figure. 5.20 : Spectrogram of multipath frequency peak (Fig. 5.19) for wet/old (red), medium (gray), and dry/fresh (blue) snows.

In Fig. 5.21, I plot the correlation between peak power strength and deviation of snow depth estimated by GPS from the AMeDAS ground truth for all the observed data. We can see weak negative correlation between these quantities. Next I estimated the coefficient in the calibration equation (deviation is expressed as a linear function of peak power) by least-squares method as shown in Fig.5.21 as blue lines.

[Calibration equation]

(L4) : Correction (m) = $-0.00558 \times$ (peak power) + 0.130 (5.1)

(SNR) : Correction (m) = $-2.0288 \cdot 10^{-5} \times$ (peak power) + 0.113 (5.2)

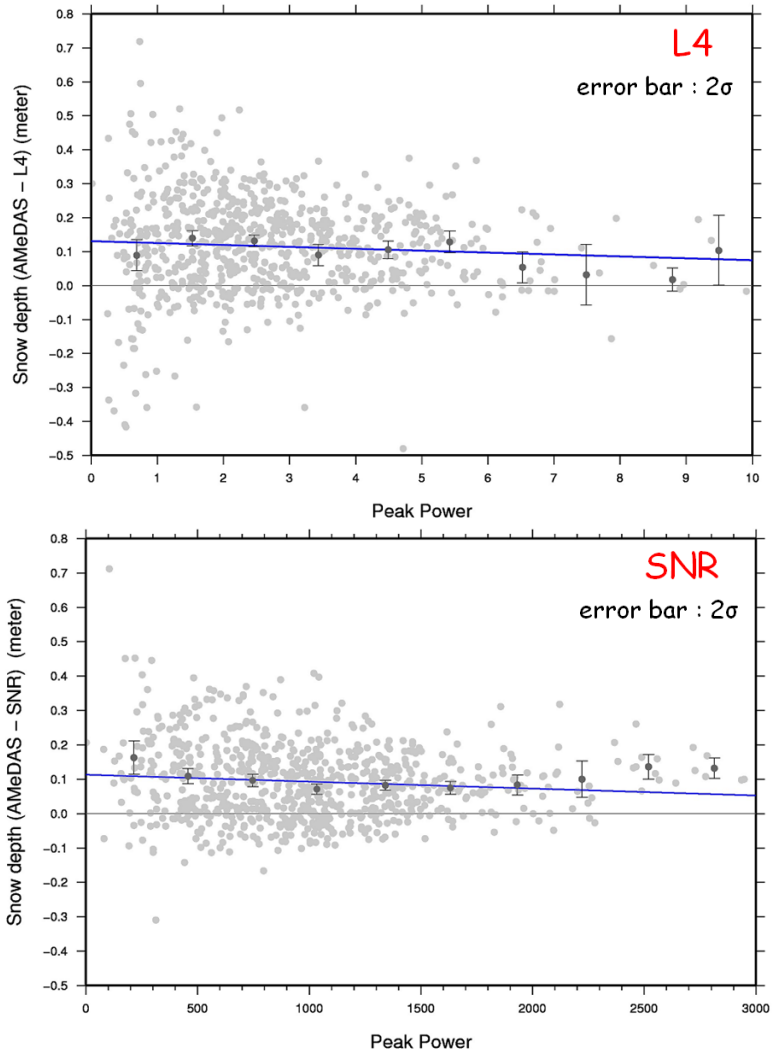

Figure. 5.21 : Correlation between peak power strength (horizontal axis) and snow depth deviation of GPS/L4 (above) and GPS/SNR (bellow) from AMeDAS (vertical axis). Gray circles show all the daily data. Black circles with 2 sigma error bars show averages taken for intervals of 1 (L4) and 300 (SNR) in the units of the horizontal axis. Calibration lines (blue lines) are determined by least-squares method.

*2　Penetration depth

Penetration depth is the index showing how long microwave can penetrate snow (Fig. 5.22). Penetration depth (L_p) can be expressed as

$$Lp(\varepsilon_r, \varepsilon_i, \lambda_0) = \frac{\lambda_0}{4\pi\sqrt{\varepsilon_r}}\left[\frac{1}{2}\left(\sqrt{1+\left(\frac{\varepsilon_i}{\varepsilon_r}\right)^2}-1\right)\right]^{-\frac{1}{2}} \quad (5.3)$$

, where ε_r is the real part of complex permittivity, ε_i is the imaginary part of that, and λ_0 is a microwave length (L2：0.24 m) (Iizaka, 1998). For the snow, ε_r is 2, ε_i is 0.1, and so L_p becomes 0.54 (m).

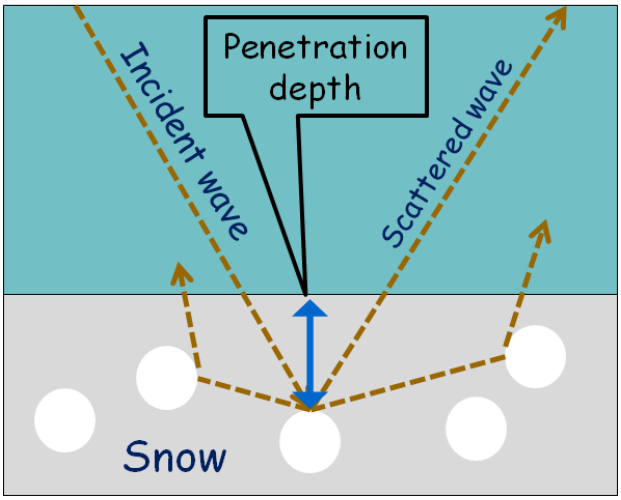

Figure. 5.22：Diagram of penetration depth

5.4 Result obtained by single satellite data after body scattering correction

The following figures (Figs. 5.23-38) show the same snow depth time series as the results shown in Figs. 5.1-16 but after the body scattering correction with the calibration equation (Eq. 5.1 for L4 and Eq. 5.2 for SNR). I applied the correction when original snow depth data is larger than 10 cm.

Results of L4

In Figs. 5.23-30 (top), I show time series of daily snow depth measurements obtained with multipath signatures in L4 after the body scattering correction. In all the figures, I gave the raw time series at the top and the smoothed time series (running averages over three consecutive days) at the bottom. As a whole, the GPS snow depth data became closer to the AMeDAS data than before.

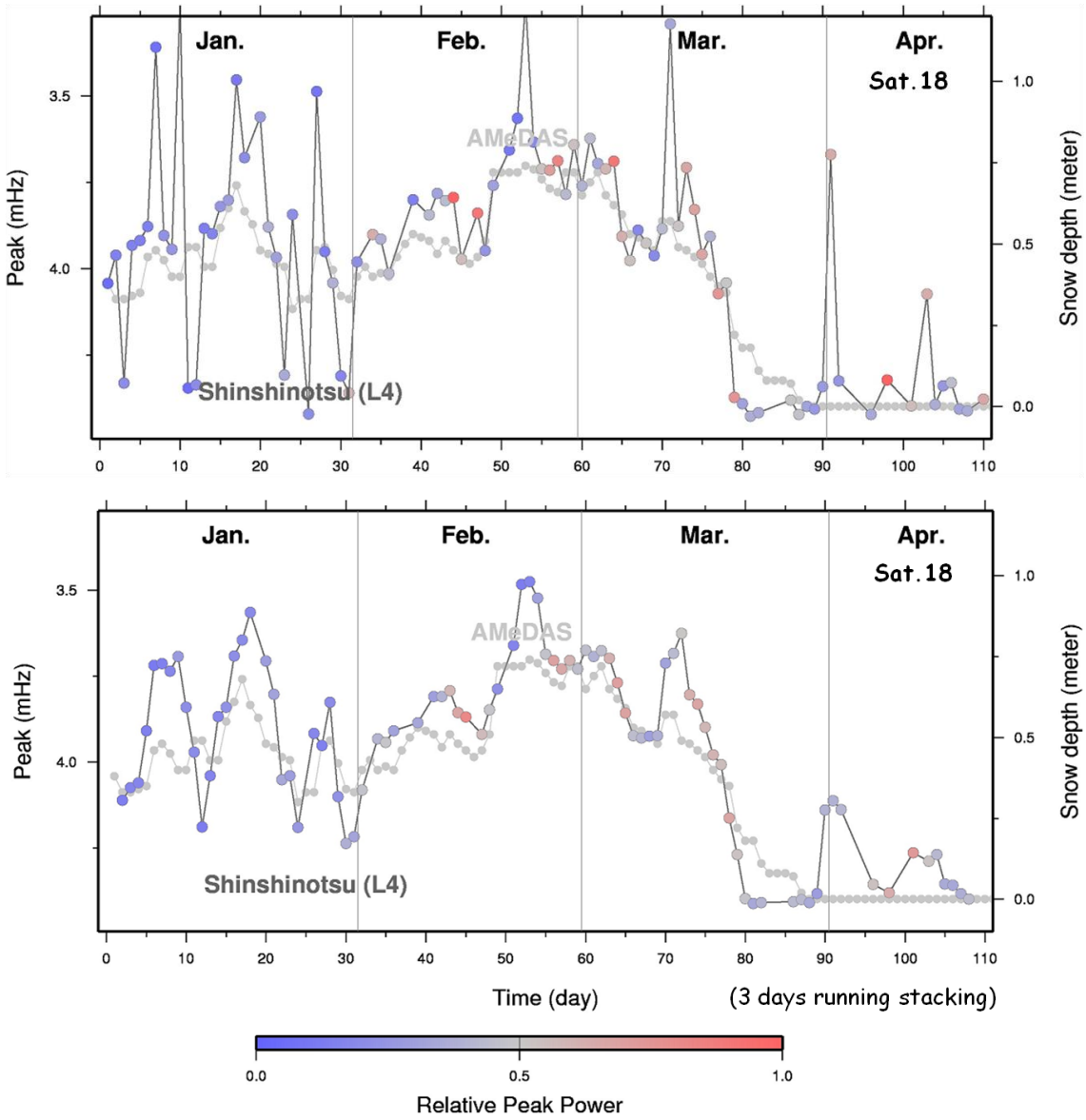

Figure. 5.23 : Raw (above) and 3 days running average (below) time series of snow depth obtained by analyzing multipath signature of the Sat.18 data before it sank. Body scattering correction has been applied. AMeDAS snow depth time series are shown by gray circles. Color scale shows multipath frequency relative peak power.

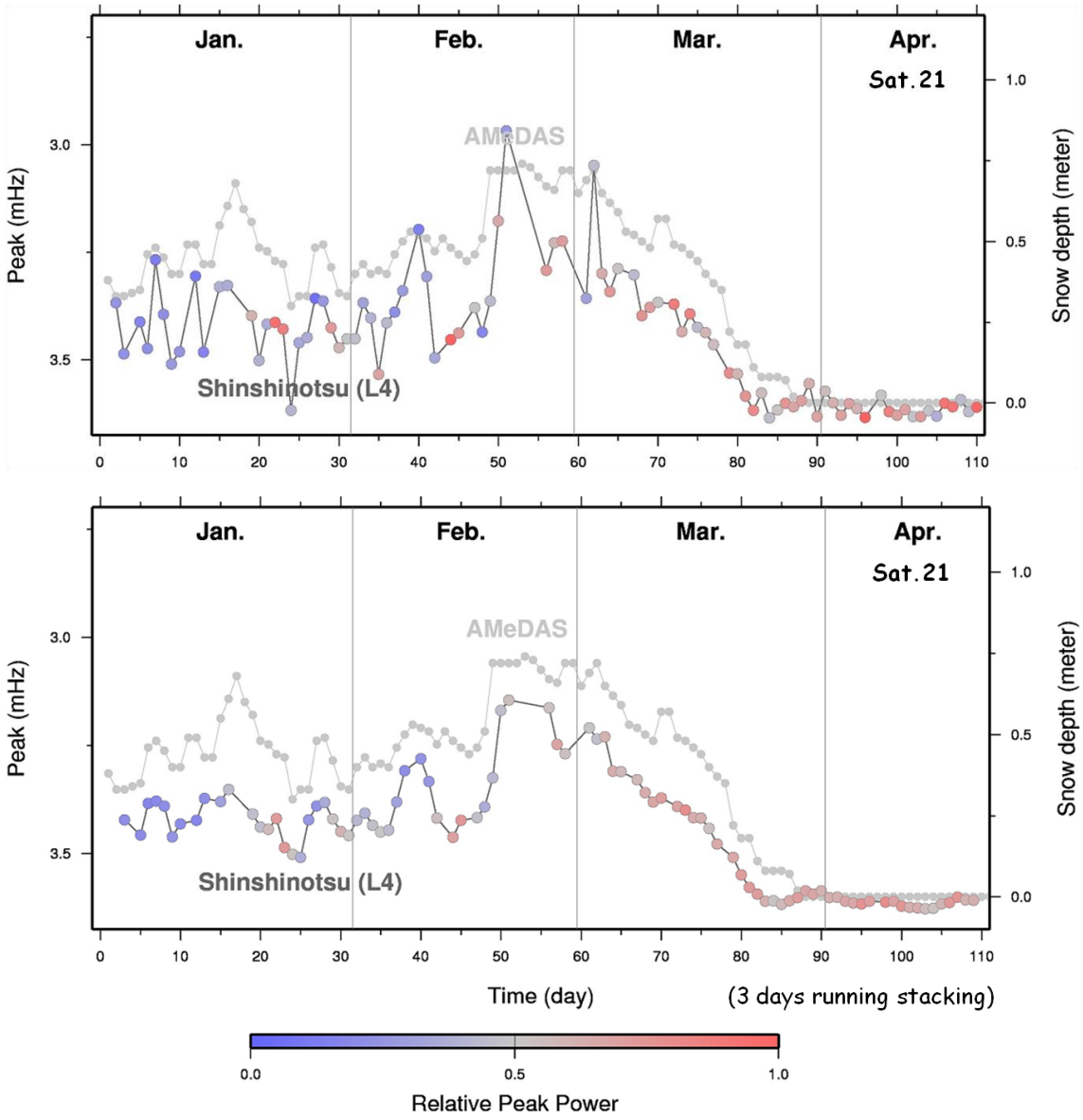

Figure. 5.24 : Same as Fig. 5.23, but data are from Sat.21 before the satellite sank.

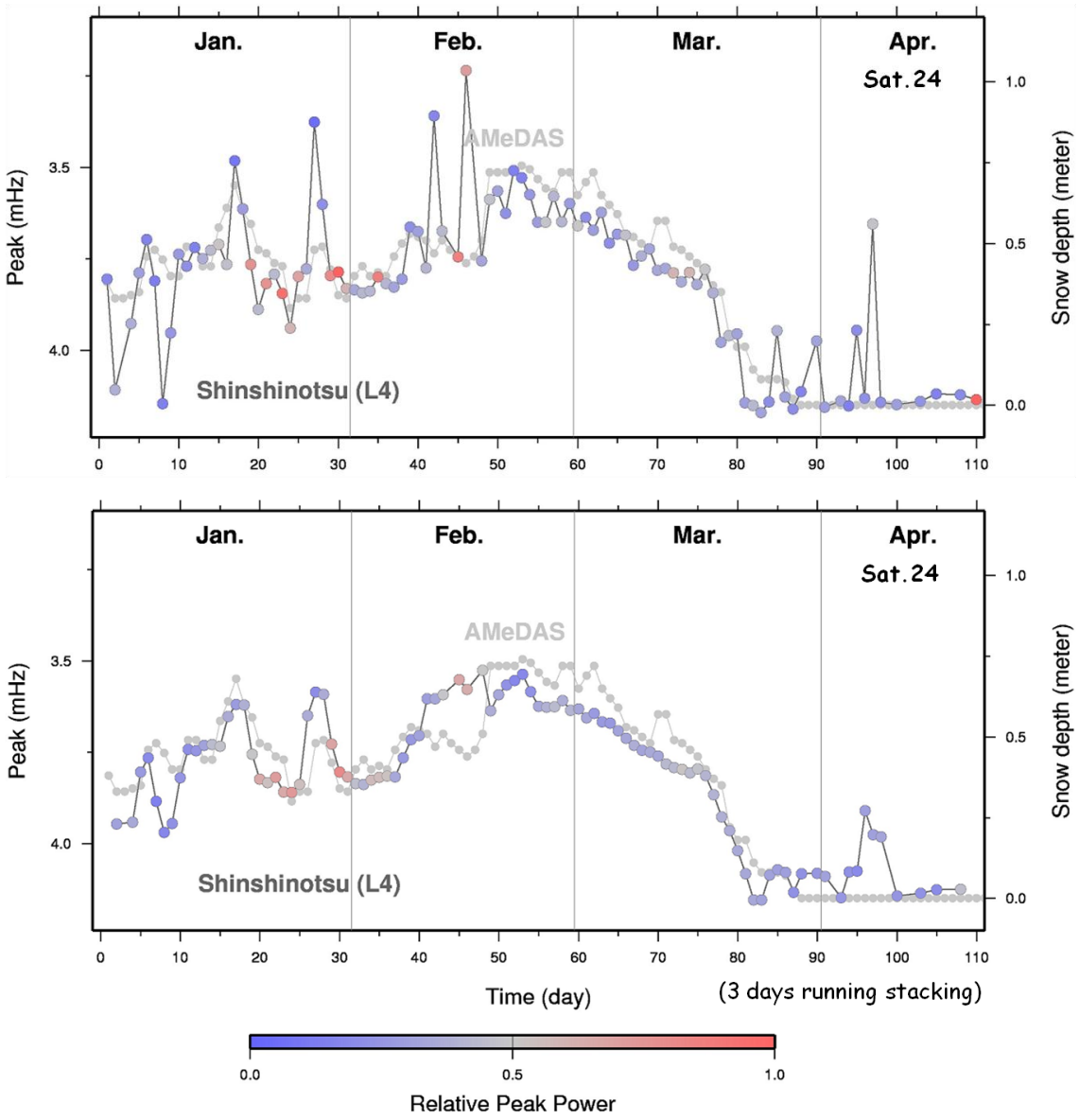

Figure. 5.25 : Same as Fig. 5.23, but I used Sat.24 data before it sank.

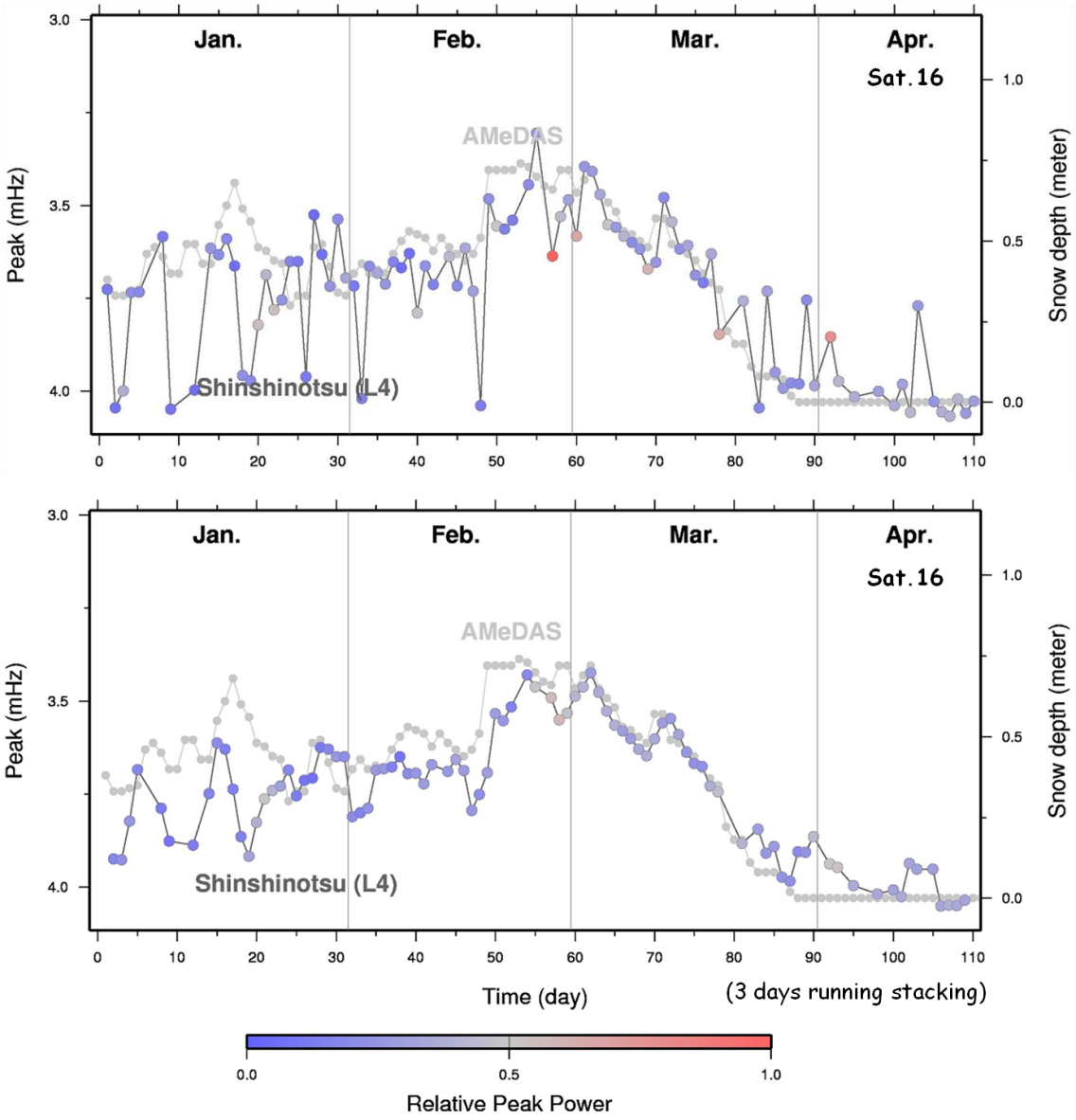

Figure. 5.26 : Same as Fig.5.23. I used Sat.16 data after it rose.

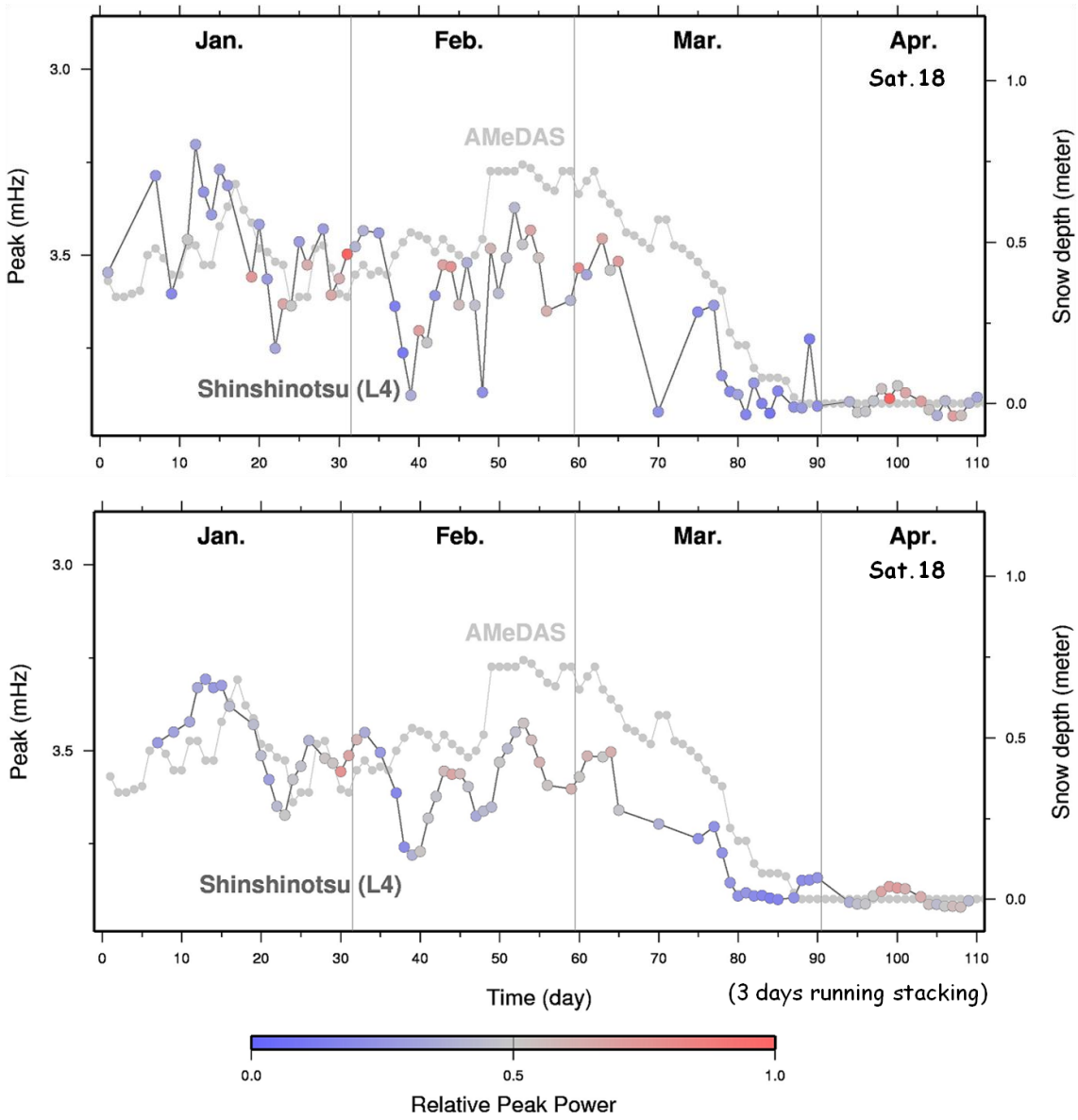

Figure. 5.27 : Same as Fig.5.23. I used Sat. 18 data after it rose.

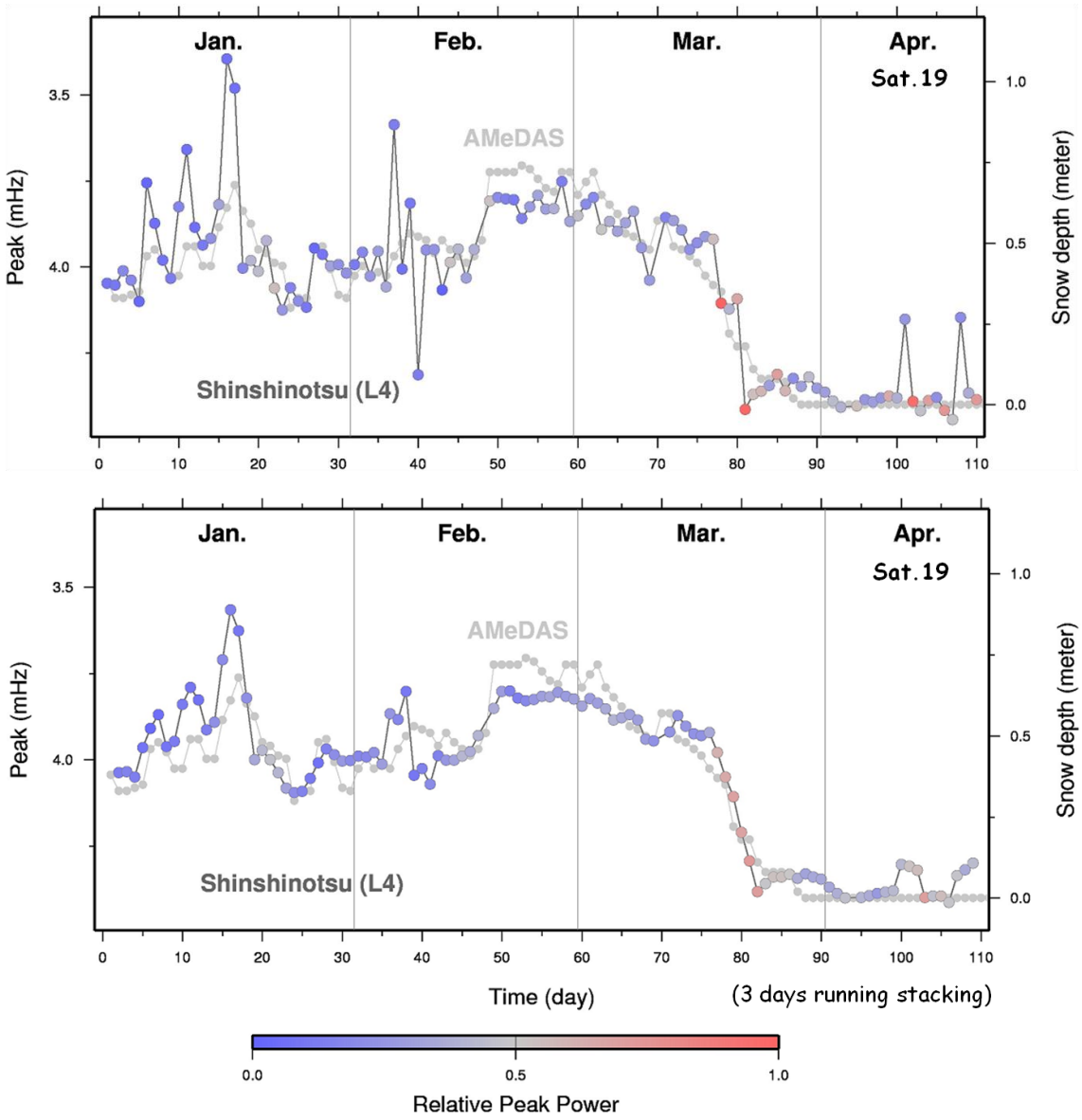

Figure. 5.28 : Same as Fig. 5.23. I used Sat.19 data after it rose.

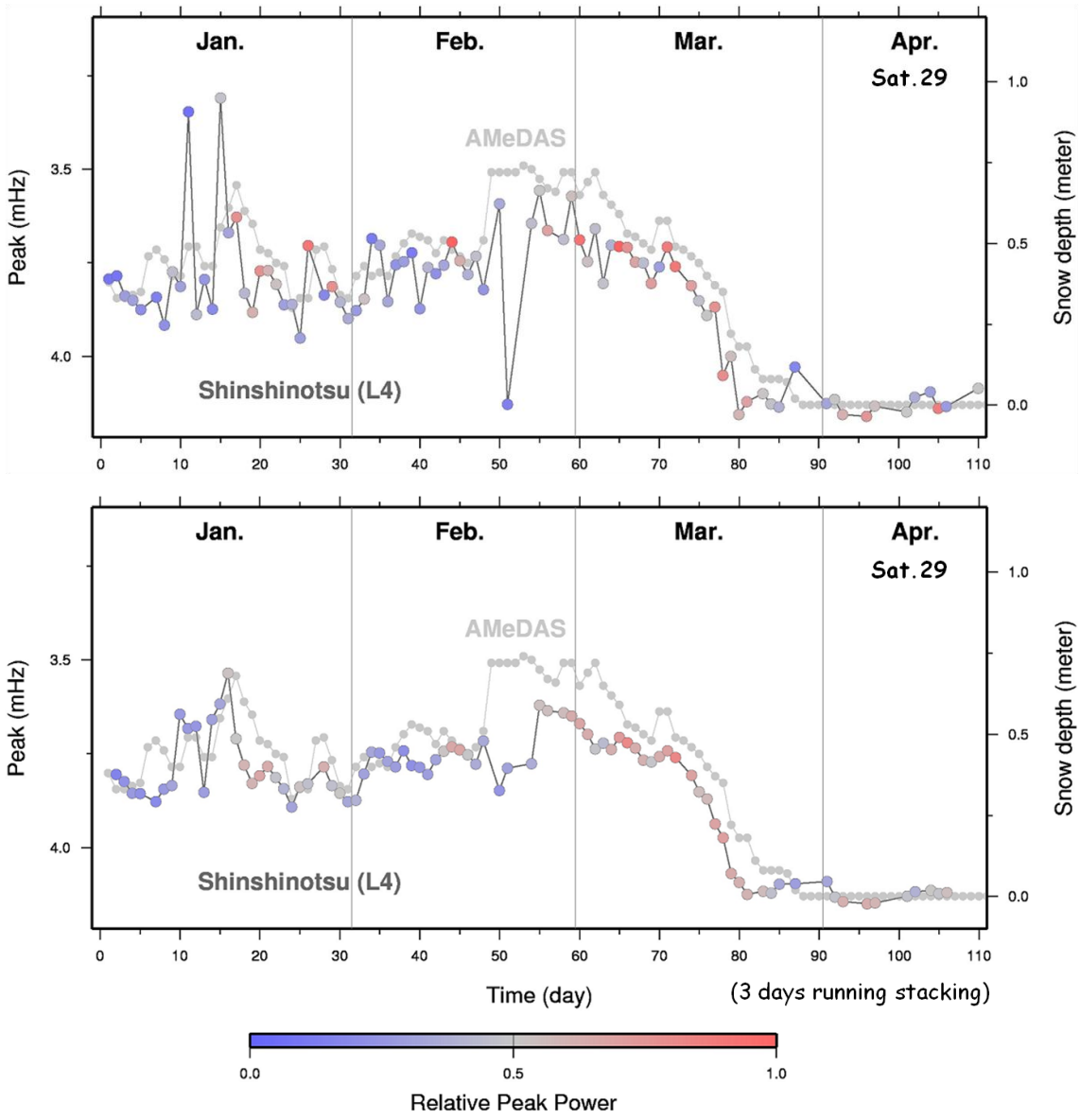

Figure. 5.29 : Same as Fig.5.23. I used the Sat.29 data after it rose.

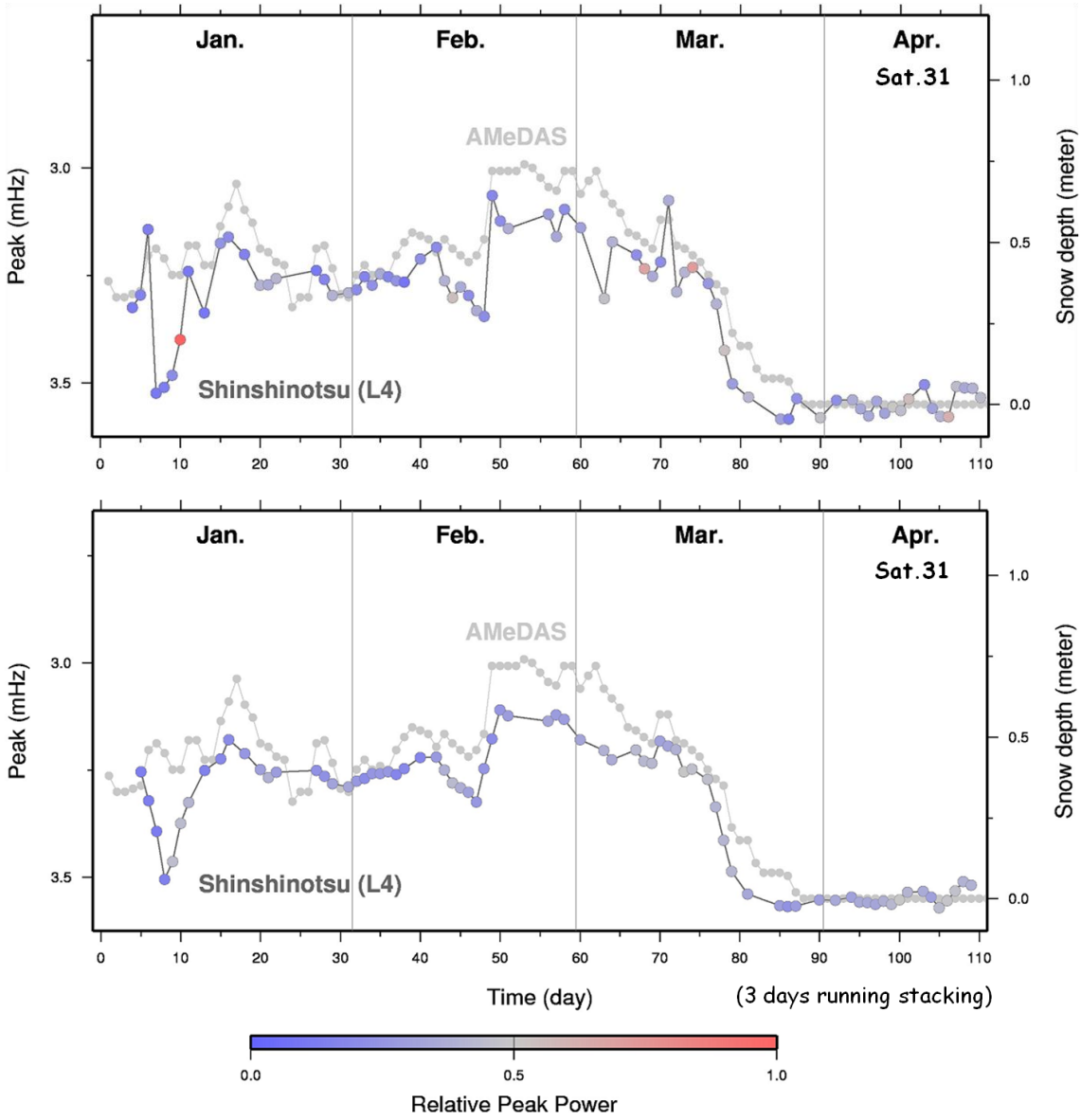

Figure. 5.30 : Same as Fig.5 23. I used the Sat.31 data after it rose.

Results by SNR

SNR snow depth data were corrected for body scattering effects in a similar way to L4. Again, the snow depth data by GPS became closer to the AMeDAS data by the correction.

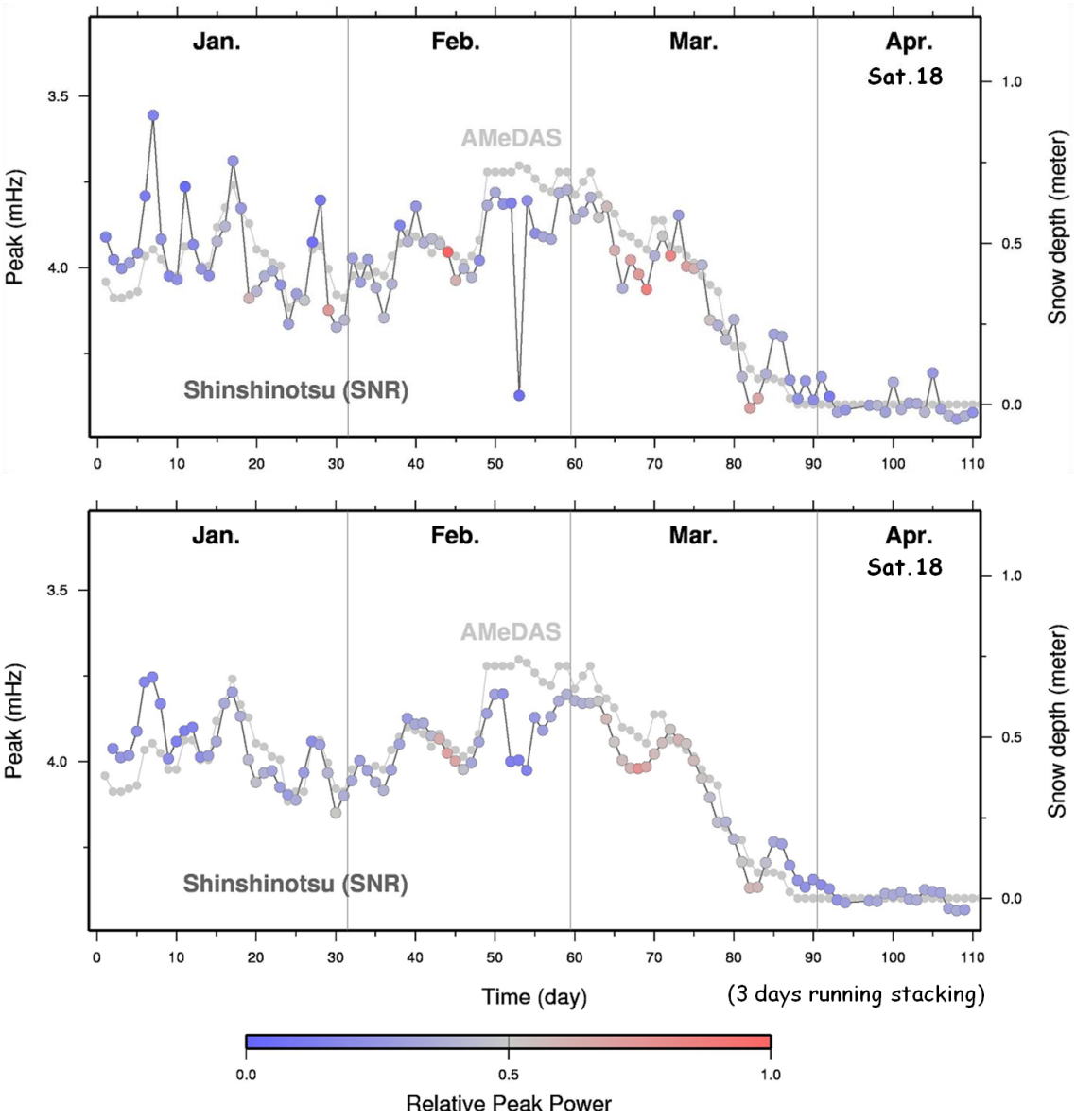

Figure. 5.31 : Raw (above) and 3 days running average (below) of the snow depth time series obtained by analyzing the multipath signatures in the SNR data from Sat.18 before it sank. Body scattering correction has been applied. The AMeDAS snow depth time series are shown by gray circles. Color scale shows multipath frequency relative peak power.

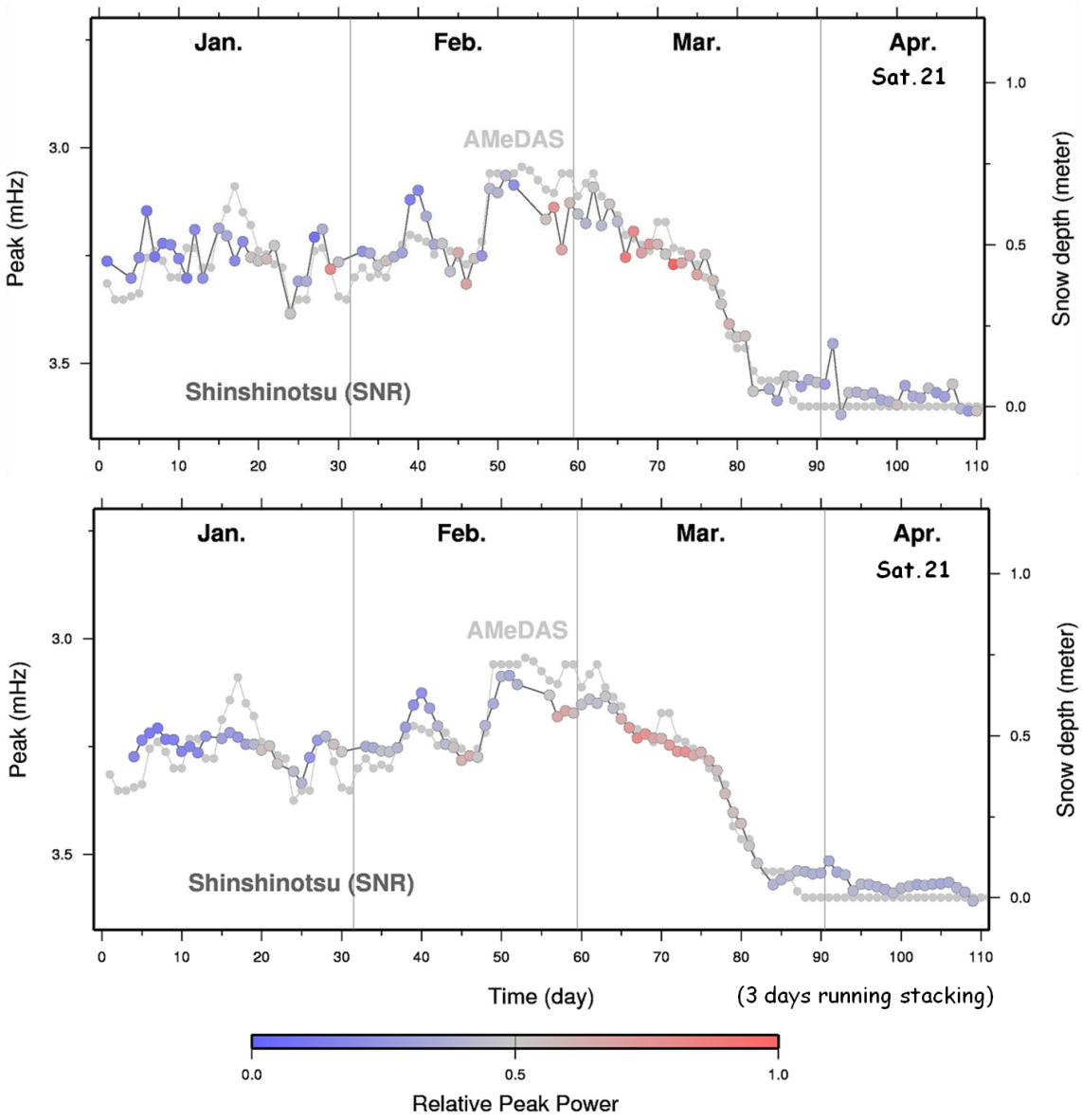

Figure. 5.32 : Same as Fig. 5.31. I analyzed data from the Sat.21 data before it sank.

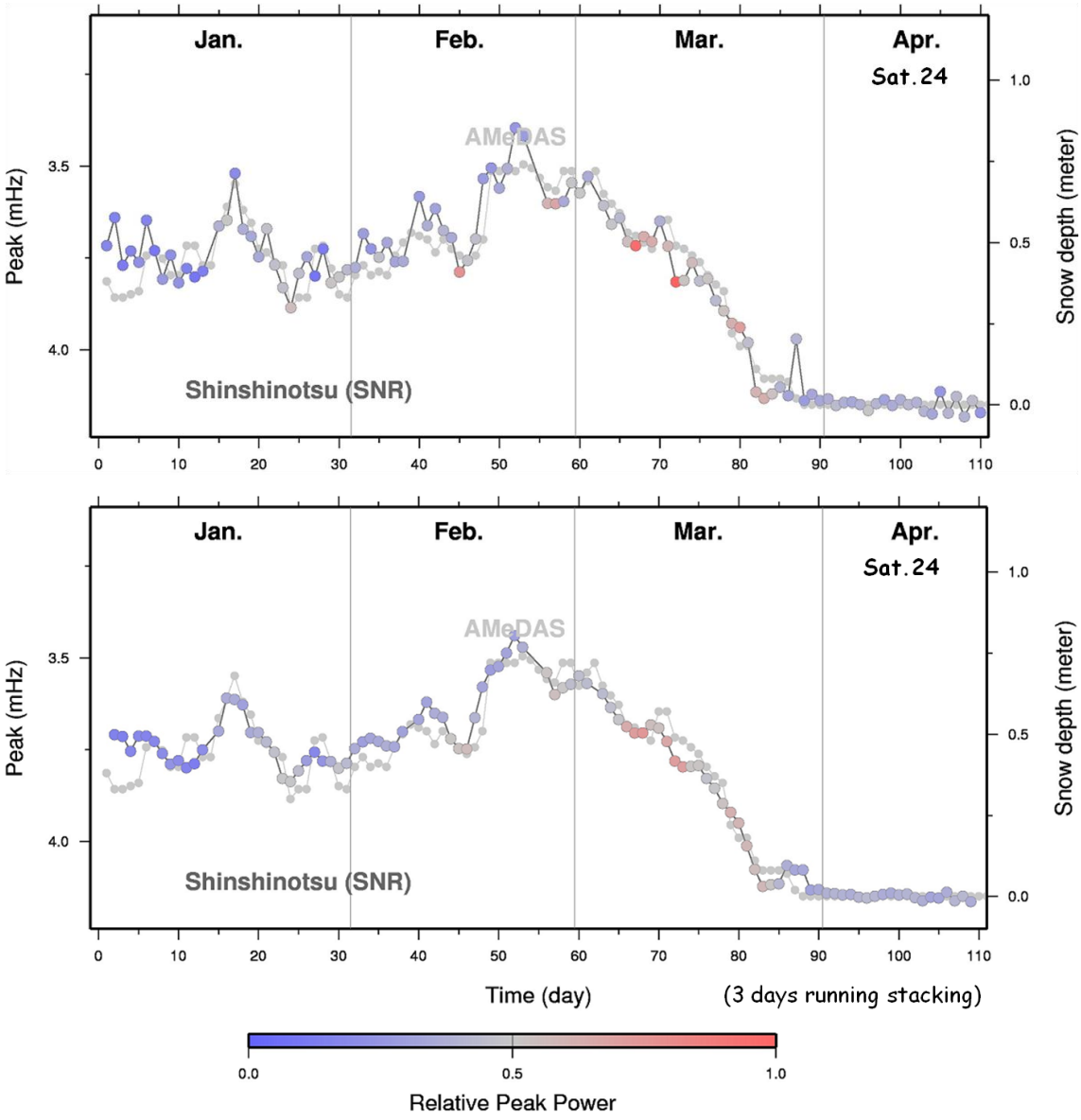

Figure. 5.33 : Same as Fig. 5.31. I used the Sat.24 data before it sank.

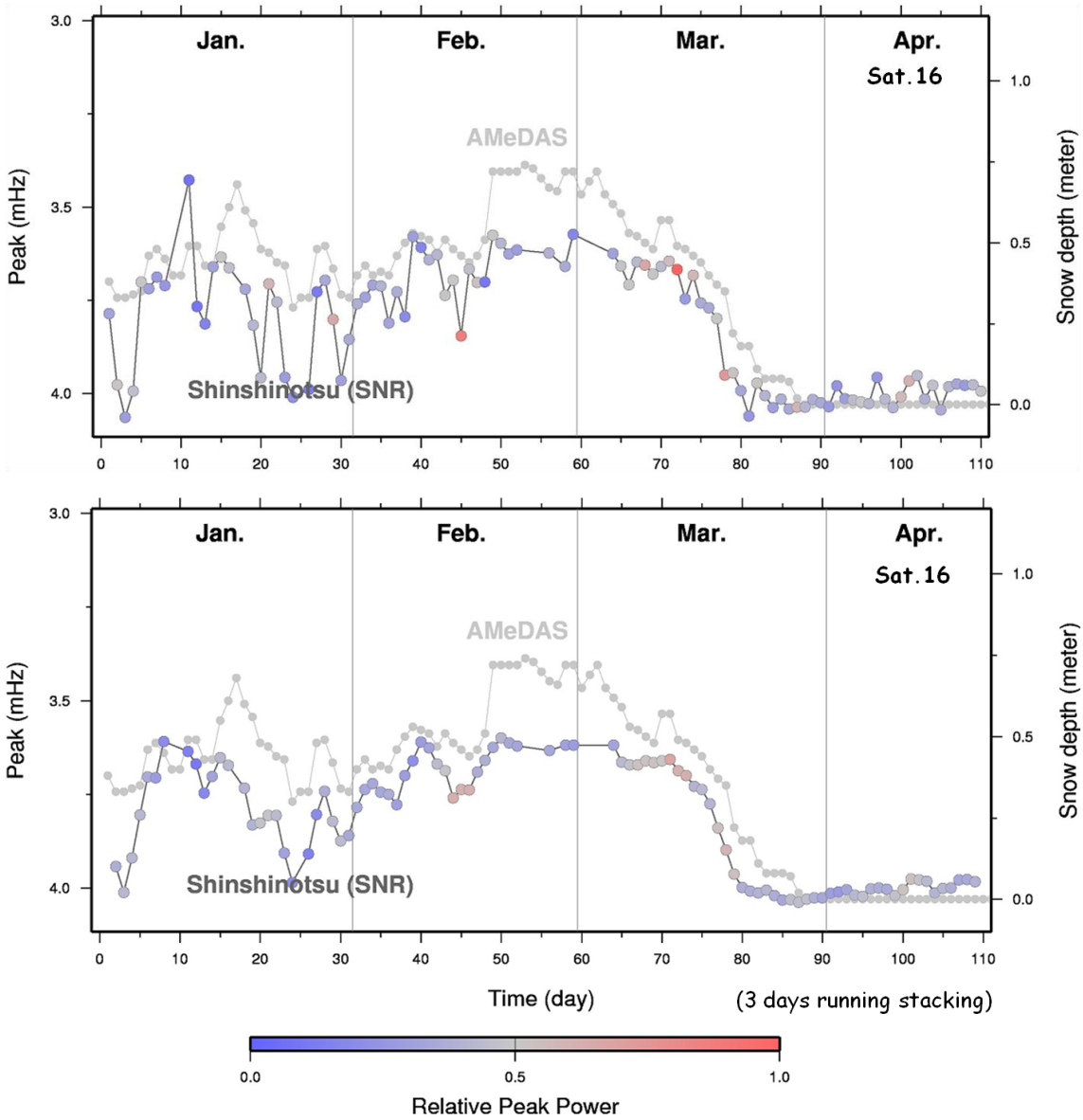

Figure. 5.34 : Same as Fig. 5.21. I used the Sat.16 data after it rose.

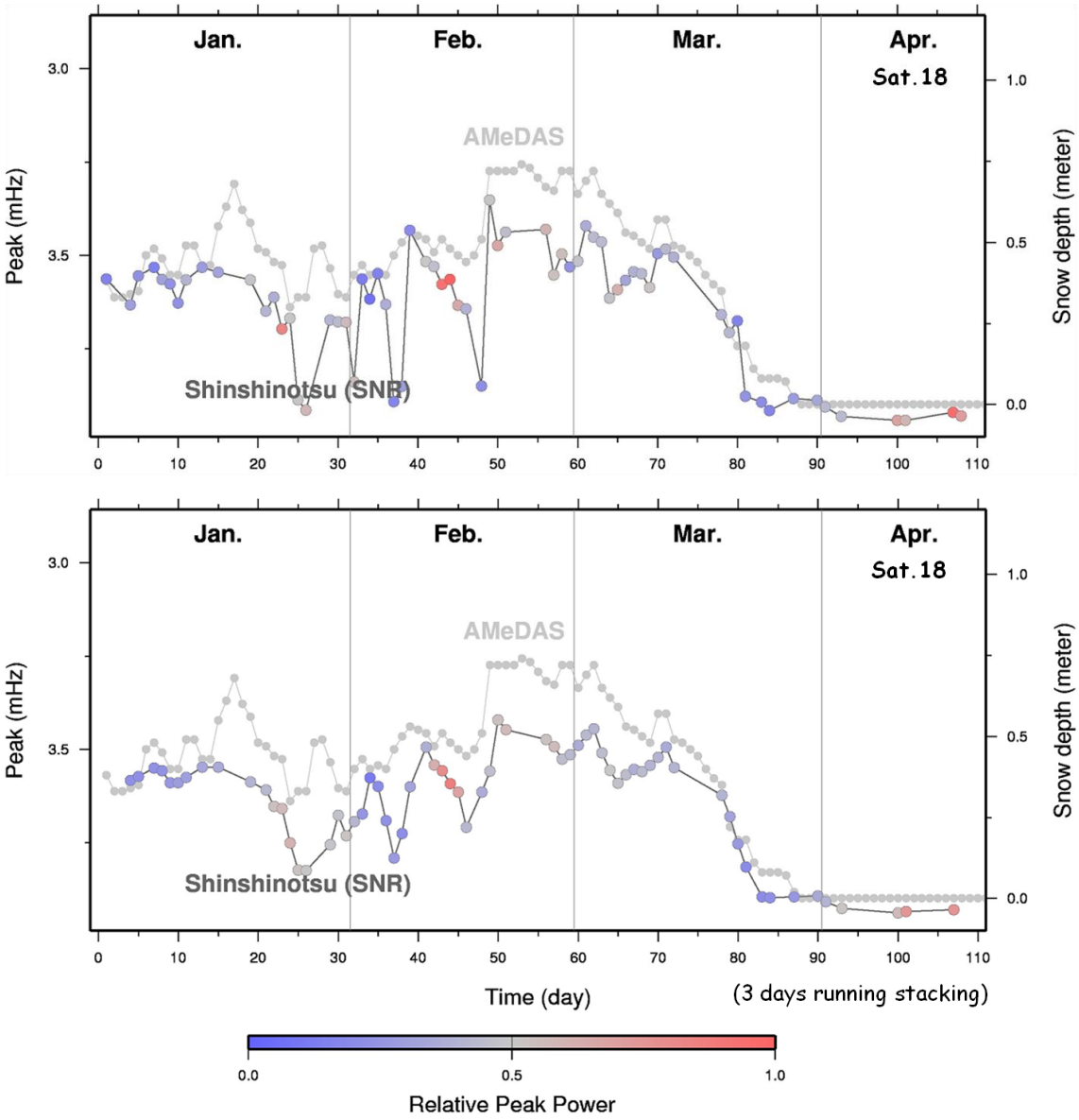

Figure. 5.35 : Same as Fig. 5.31. I used the Sat.18 data after it rose.

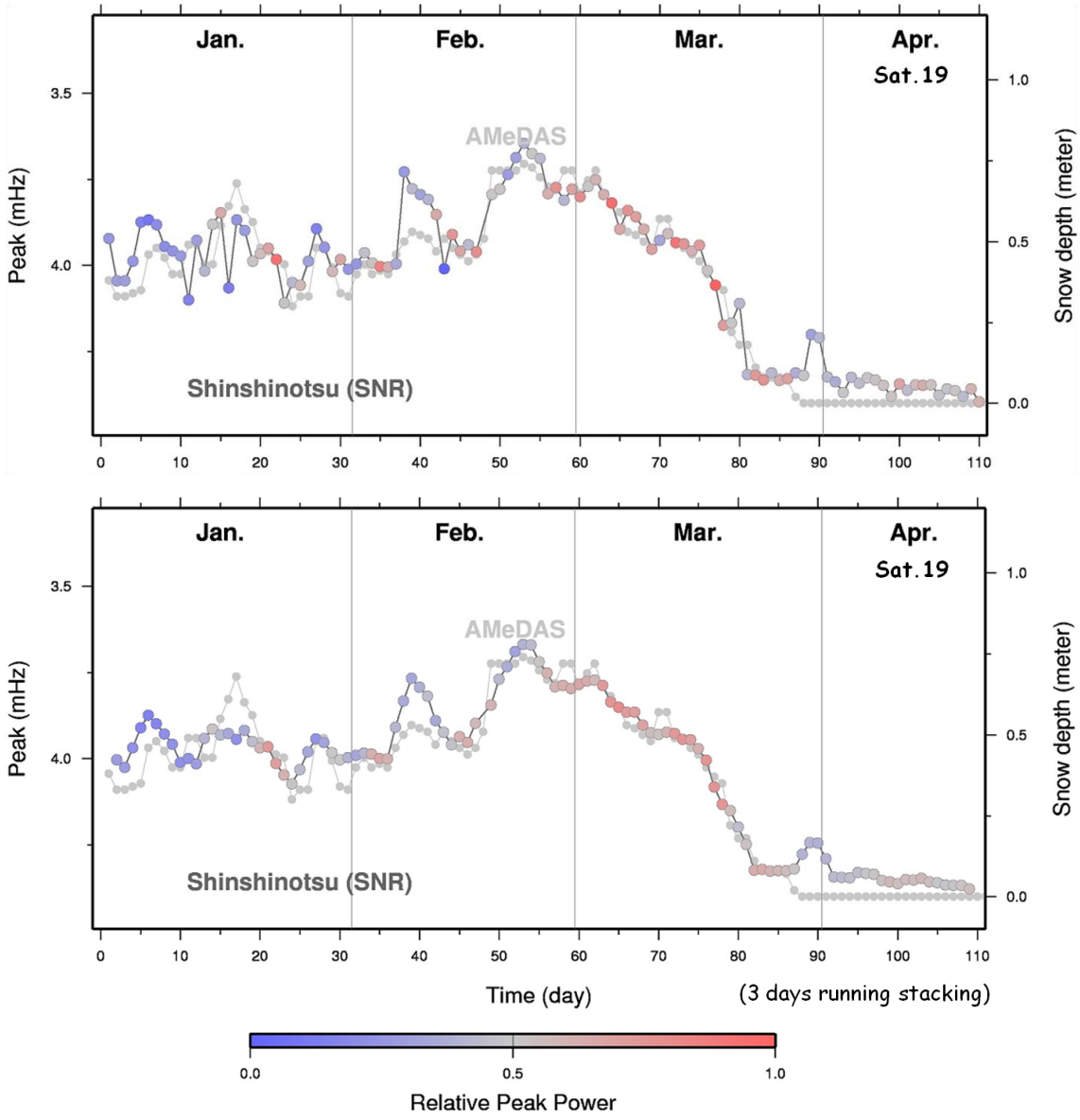

Figure. 5.36 : Same as Fig. 5.31. I used the Sat.19 data after it rose.

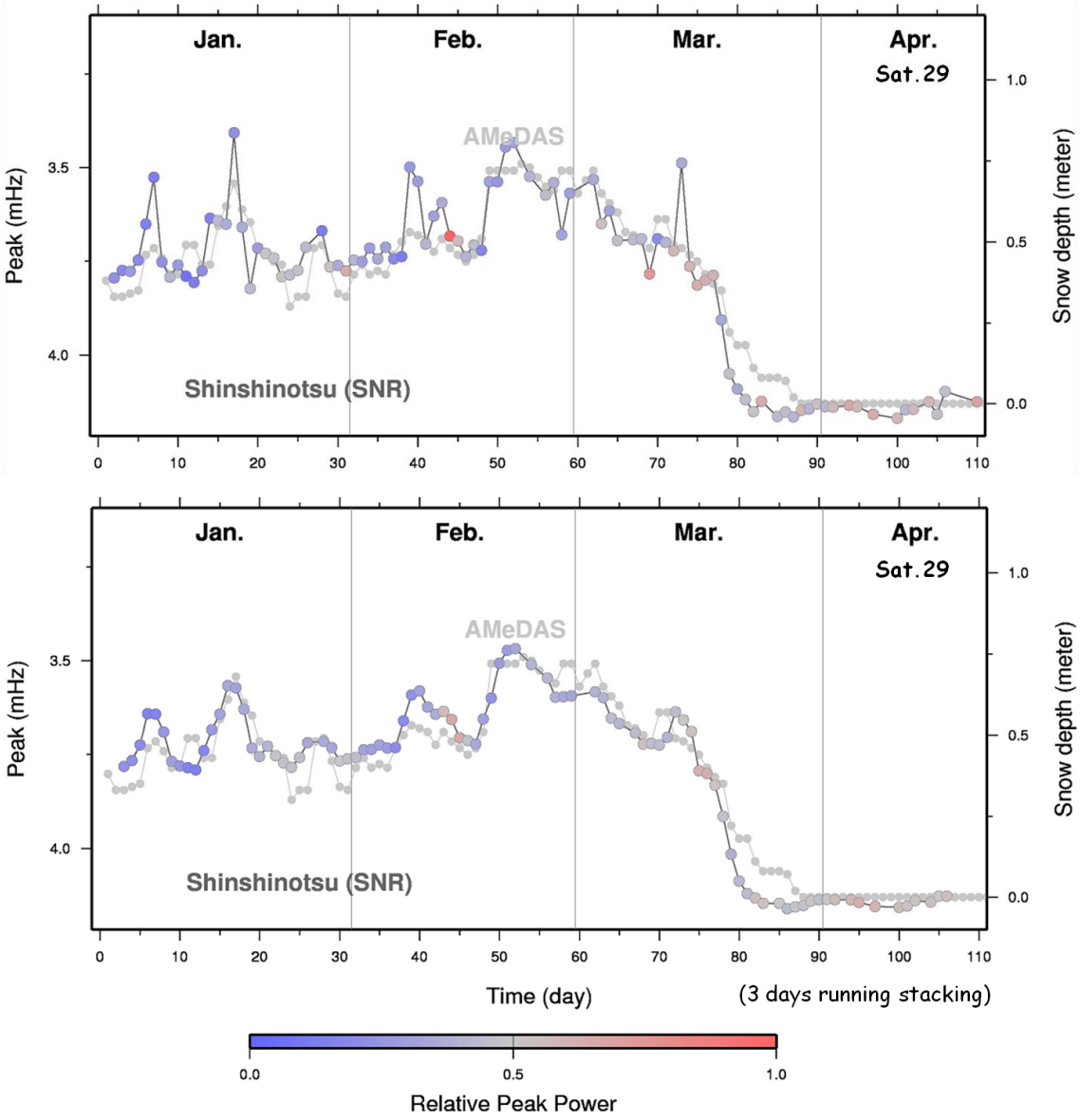

Figure. 5.37 : Same as Fig. 5.31. I used the Sat.29 data after it rose.

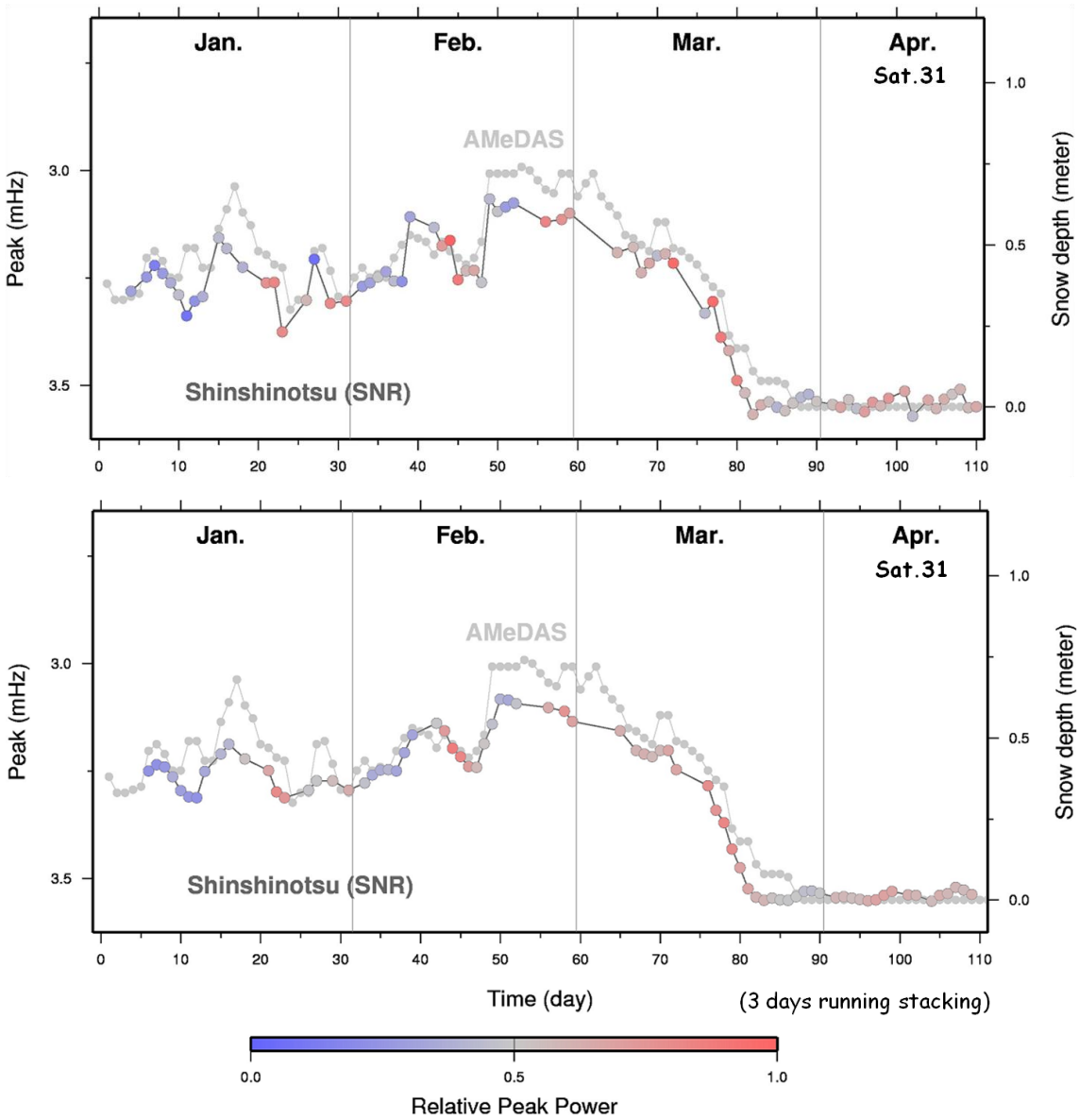

Figure. 5.38 : Same as Fig. 5.31. I used the Sat.31 data after it rose.

5.5 Results from multiple satellites after body scattering correction

I show snow depth time series obtained as weighted averages (weights were determined using the peak power strength) of data inferred from multipath signatures in L4 (Fig.5.39) and SNR (Fig.5.40) of all the satellites (body scattering correction was applied). In both figures, top panels show daily estimates and bottom panels show the time series smoothed by taking running averages over three consecutive days. By the body scattering correction, the agreement between the GPS and AMeDAS data has been much improved. RMS (Root Mean Square) between GPS (L4 and SNR, smoothed time series) and AMeDAS during this observing period is 0.0735 (m) and 0.0542 (m), respectively.

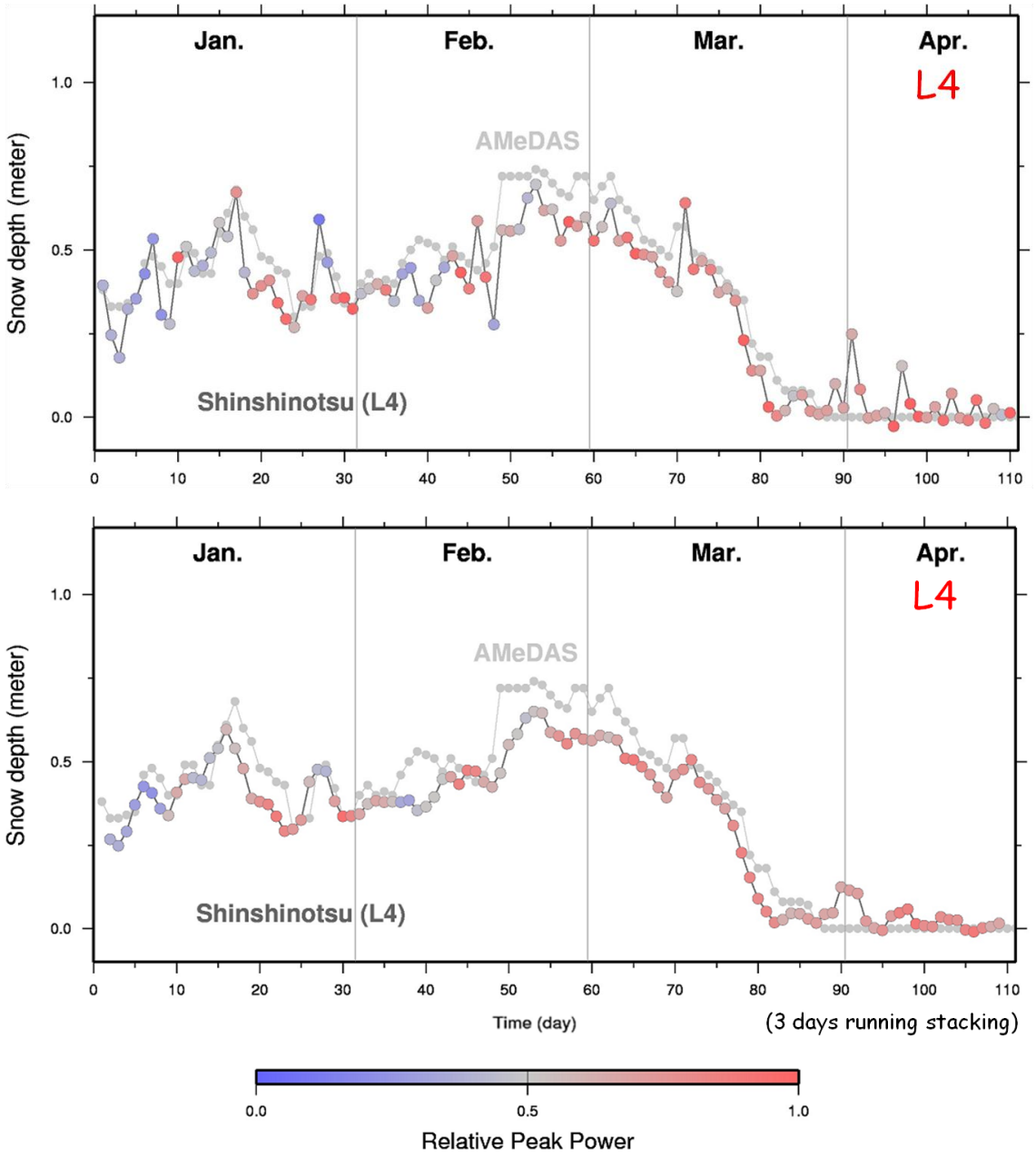

Figure. 5.39 : Snow depth time series (top: daily, below : 3 days running average) obtained as averages of snow depth values inferred from all the satellites. Here, L4 data are used and body scattering correction has been applied. The AMeDAS snow depth time series are shown with gray circles. Color scale shows multipath frequency relative peak power.

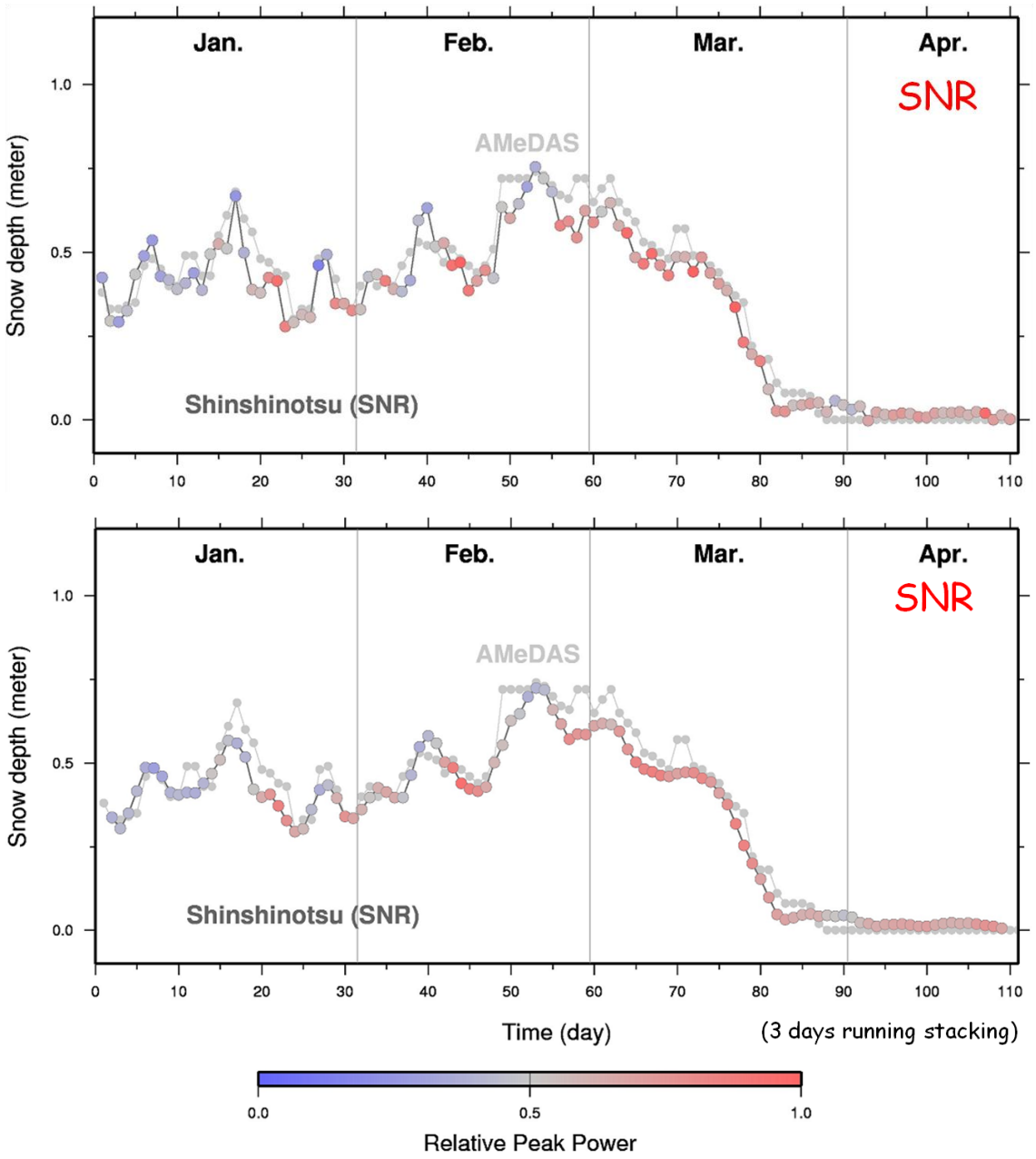

Figure. 5.40 : The same as the Fig. 5.39, except that SNR was analyzed instead of L4.

6 Conclusion

It was shown that GPS and AMeDAS data agree with each other fairly well in Chapter 5. Therefore, I found that the snow depth meter by observing L4 multipath of GPS was possible, under the condition which a GPS antenna stands in an open ground.

There are only ~300 AMeDAS sensors which can measure snow depths in northern Japan. On the other hand, there are >1000 GPS antennas of GEONET stations throughout Japan. It might be possible that snow depth data obtained by GPS complement the AMeDAS snow depth meter network. Also we can measure snow depths by using GPS in countries where no snow depth sensors are available. Thus, it is important for meteorological, climatological, hydrological and glaciological points of view to be able to know snow depths by analyzing data from GPS stations installed for geodetic purposes.

Also, I compared the snow depth results obtained by analyzing L4 and SNR. They were of comparative accuracies, because both RMS (Root Mean Square) between GPS (L4 and SNR) and AMeDAS are very small. The two observables are quite different, i.e. SNR is derived from the fluctuation of intensities of the received microwaves, while L4 is derived from the phase changes of the received microwaves. Therefore, it is interesting that the snow depth results from L4 and SNR agreed with each other.

In 2009, the GEONET RINEX data files started to include SNR data, but RINEX files from many GPS networks worldwide still do not include SNR data. Therefore, when we measure snow depth by these GPS networks, L4 can be used as a proxy of SNR because every RINEX file includes L1 and L2 data.

Finally, this GPS snow depth sensor by L4 can be applied to measure other quantities as well as SNR. For example, we can measure soil moisture by using L4 as Larson et al. (2008) demonstrated by analyzing amplitudes of SNR fluctuations. It is also possible to use L4 multipath frequency peak power for this purpose because it also changes according to the reflectivity of the ground surface. We may be able to observe growth of vegetation (e.g. rice, corn) remotely by using L4 as Small et al. (2010) did by using SNR. This is important especially in Japan where rice is the staple food of the people.

7 References

Eloségui, P. et al., 1995, Geodesy using the Global Positioning System: The effects of signal scattering, J. Geophys. Res., 100, 9921.

Hino, M., 1984, Spectrum analysis, Asakura-shoten.(in Japanese)

Iizaka, J., 1998, Handbook of Synthetic Aperture Radar Images – New technique in Earth's environment measurement, Asakura-shoten (in Japnese)

Larson, K. et al., 2008, Using GPS multipath to measure soil moisture fluctuations: Initial results, GPS Solut., 12(3), 173-177, doi:10.1007/s10291-007-0076-6

Larson, K. et al., 2009, Can we measure snow depth with GPS receivers?, Geophys. Res. Lett., 36, L17502, doi:10.1029/2009GL039430

Small, E. et al., 2010, Sensing vegetation growth with reflected GPS signals, Geophys. Res. Lett., 37, L12401, doi:10.1029/2010GL042951

Tsuji, H., 1999, GPS meteorology, Chapter 1, Principle of GPS, Kisho-Kenkyu-Note, No. 192, Met. Soc. Japan. (in Japanese)

AMeDAS data [http://www.jma.go.jp/jp/amedas/]

GEONET data [http://terras.gsi.go.jp/gps/geonet_top.html]

謝辞

大学に入学してから 6 年間、この修士論文を完成させるまでお世話になった皆様にここで改めて感謝の意を表したいと思います。

まず指導教官の日置幸介教授には、研究の進め方や学会発表に至るまで非常に多くのアドバイスを頂きました。特に、研究の進め方に関しては一つ一つ順を追って解決していくやり方、学会の発表に関してはスライド資料の見せ方やポスターの発表の方法と、これから物事を考える時や社会で出て行く上でもとても役立つことを勉強させて頂きました。また、彗星・地球自由振動・ミサイルそして本修士論文である積雪深度測定に至るまで様々な題材を扱うことができた GPS-TEC の研究を提示して頂いたことにも感謝しております。そもそも私がこの研究室に配属したいと思うきっかけになったのも、分属説明会で日置教授がおっしゃった「宇宙測地学は色々なテーマの研究ができる」という言葉でした。やってみたい研究対象が一つに決まらずいろんなことをやってみたいと迷っていた私にはもってこいの研究室で、この 3 年間はまさにそれを実現できたと思っています。

次に、宇宙測地学研究室の古屋正人準教授、そして固体系ゼミの小山順二教授、蓬田清教授、吉澤和範准教授、勝俣啓准教授、山田卓司助教には、ゼミの発表において今後の研究に役立つ助言して頂きました。特に学会前の発表練習にも参加して頂き、訂正すべき箇所を指摘して頂くことによって、本番に余裕を持って臨むことができ安心して発表を行うことができました。そのおかげで日本測地学会の発表では「学生による講演会優秀発表」を頂くことができ、誠に感謝しております。

そして、以上の先生方を含め学士から修士課程にかけて参加した講義の先生方には、物理数学・地球物理分野の基礎から応用まで教えて下さったことにより、高校の頃から興味を持っていた物理・地球・宇宙に関しての知識をより深めることができ、研究を進めることができたと思っています。

最後に、松尾功二先輩をはじめとする研究室の学生の皆様には些細なことから研究に関することまで気兼ねなく質問させて頂き、スムーズに研究を進めることができました。

以上の方々のおかげで、私の研究生活が充実したものになったと思っています。本当にありがとうございました。